Tetrahedron: *Asymmetry* 22 (2011) 2085–2098

Contents lists available at SciVerse ScienceDirect

Tetrahedron: *Asymmetry*

journal homepage: www.elsevier.com/locate/tetasy

Absolute configuration assignment of 3-oxindolylacetyl-4-phenyloxazolidinone derivatives

Oscar R. Suárez-Castillo [a,*], Myriam Meléndez-Rodríguez [a], Luis E. Castelán-Duarte [a], Erick A. Zúñiga-Estrada [a], Julián Cruz-Borbolla [a], Martha S. Morales-Ríos [b], Pedro Joseph-Nathan [b]

[a] *Área Académica de Química, Universidad Autónoma del Estado de Hidalgo, Mineral de la Reforma, Hidalgo 42184, Mexico*
[b] *Departamento de Química, Centro de Investigación y de Estudios Avanzados del Instituto Politécnico Nacional, Apartado 14-740, Mexico DF, 07000, Mexico*

ARTICLE INFO

Article history:
Received 21 October 2011
Accepted 30 November 2011
Available online 20 January 2012

ABSTRACT

The straightforward determination of the absolute configuration of 2-oxo-3-indolylacetic acid derivatives **5a**–**e**, based on analysis of the ^{1}H NMR spectra of their oxindolylacetyl-phenyloxazolidinones **6a**–**e**, is described. The conformational preferences for two diastereomeric amides were calculated by DFT, which matched well with the experimental results, while X-ray diffraction analysis allowed us to validate the methodology. Independent absolute configuration evidence was also obtained by vibrational circular dichroism.

1. Introduction

Substituted oxindole derivatives **1** (Fig. 1) are of considerable interest since they are natural products as well as starting materials or intermediate compounds in the total synthesis of terrestrial and marine natural products containing the furo- and pyrroloindole skeletons **2**.[1,2] Due to the optical activity of oxindole derivatives such as **1**, suitable and easy methods to assign their absolute configuration are required. As part of an ongoing effort to develop improved chiral derivatizing agents (CDAs) for determining the absolute configuration of oxindole derivatives, we have recently demonstrated that ^{1}H NMR spectroscopy could be a useful tool for establishing these assignments in chiral 2-(2-oxo-3-indolyl)acetetamide derivatives **3** (Fig. 2) using enantiomerically pure phenylethylamine (FEA) as a CDA.[3] Experimental data and DFT calculations demonstrated that the phenyl ring of FEA shields the *N*1–R^1 group in the (3*R*,11*R*)-**3** derivatives, whereas, in the (3*S*,11*R*)-**3** diastereomers, the shielded group is C3–R^2. Thus, the $\Delta\delta^{RS}$ parameter allows us to assign the absolute configuration in diastereomers **3** as shown in Figure 2.

Herein we report that (*R*)- or (*S*)-phenyl-2-oxazolidinone **4** could be a reliable CDA for the absolute configuration assignment of chiral 2-(2-oxo-3-indolyl)acetic acid derivatives regardless of the substituents at the *N*1- or C3-positions (Scheme 1). One advantage of the present methodology is that once the absolute configuration at C3 in the oxindolyl moiety has been achieved, the CDA could be recovered after hydrolysis of the corresponding oxazolidinone. Although aryloxazolidinones are versatile chiral auxiliaries and have been used for the synthesis of indole derivatives, enolate alkylations, Michael additions, β-lactams, alkene acylation, cyclopropanations, Wittig olefination, and Diels–Alder reactions,[4] their use as a CDA has scarcely been explored. Pirkle and Simmons have achieved the absolute configuration assignment of primary amines by ^{1}H NMR via the formation of allophanate derivatives in which the aryl ring causes specific shielding on the substituents of the amine[5a] moiety, while Pridgen and De Brosse have carried out the relative stereochemical assignments of some *N*-[α-hetero-β-hydroxy(acetoxy)-β-(substituted-phenyl)-1′-oxopropyl]-2-oxazolidinones.[5b]

2. Results and discussion

In order to evaluate the utility of (*S*)-phenyloxazolidinone **4** as a CDA for the absolute configuration assignment of the C3 stereogenic center in 2-oxo-3-indolylacetic acid derivatives **5a**–**e**,[2i,l,3,6] containing a variety of substituents at the *N*1 and C3 positions, diastereomeric oxindolylacetyl-phenyloxazolidinones **6a**–**e** were synthesized according to Scheme 1. Oxindolylacetic acid derivatives **5c**,**d** have been used as intermediates in the total synthesis of natural products.[2i,l,6a,b] A derivatization of racemic carboxylic acids **5a**–**e** into oxazolidinones was carried out by the activation of **5a**–**e** with dicyclohexylcarbodiimide (DCC) or 1-ethyl-3-(3-dimethylaminopropyl)carbodiimide (EDC) and 4-dimethylaminopyridine (DMAP),[7] followed by the reaction with phenyloxazolidinone (*S*)-**4** to give equimolar diastereomeric mixtures of (3*R*,14*S*)-**6a**–**e** and (3*S*,14*S*)-**6a**–**e**, as evidenced by ^{1}H NMR analysis of the reaction crudes, which indicated that no kinetic resolution occurred.[8] Diastereomeric phenyloxazolidinones (3*R*,14*S*)-**6a**–**e** and (3*S*,14*S*)-**6a**–**e** were easily separated by column chromatography (Table 1) to afford pure isomers with de >99% as determined by ^{1}H NMR measurements.

* Corresponding author. Tel.: +52 771 71 72000x2206; fax: +52 771 71 72000x6502.
E-mail address: osuarez@uaeh.edu.mx (O.R. Suárez-Castillo).

0957-4166/$ - see front matter © 2011 Elsevier Ltd. All rights reserved.
doi:10.1016/j.tetasy.2011.11.018

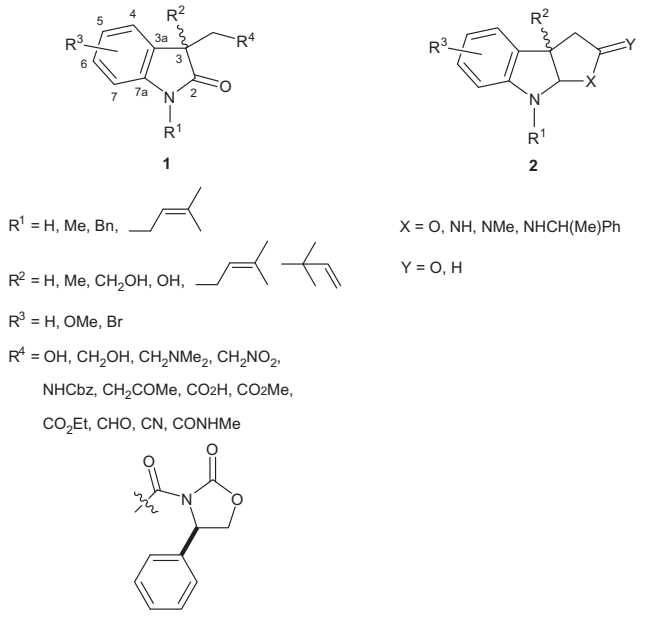

Figure 1.

The ^{1}H NMR spectra allowed discrimination of oxazolidinones (3*R*,14*S*)-**6a**–**e** and (3*S*,14*S*)-**6a**–**e** since these compounds showed large enough chemical shift differences ($\Delta\delta^{RS} = \delta_R - \delta_S$, where the *R* and *S* descriptors refer to the stereogenic C3 configuration in the oxindole moiety[3,9]) for the H4–H7, H16–H20 and H8A signals (Table 2). These significant chemical shift nonequivalences arise from the mutual diamagnetic influence of the aromatic (*S*)-oxazolidinone and the oxindole moieties on the NMR signals of their own hydrogen atoms. Diastereomeric oxazolidinones **6a** were used as representative models to evidence this fact. As shown in Figure 3 with **C** and **D**, the signals due to H4–H7 and H16–H20 showed lower chemical shift values for the (3*S*,14*S*)-**6a** isomer than for the (3*R*,14*S*)-**6a** diastereomer ($\Delta\delta^{RS}$ >0, Table 2). In the aliphatic region, remarkable $\Delta\delta^{RS}$ shifts occurred only for the C8AB system, for which the chemical shift value for H8A is higher in (3*S*,14*S*)-**6a** than in (3*R*,14*S*)-**6a**, showing $\Delta\delta^{RS}$ <0 for HA (Fig. 3, **A** and **B**, Table 2). It is worth noting that the chemical shift for the *N*1-Me and C3-Me groups are almost the same in both diastereoisomers, suggesting at first glance that substituents in those positions do not influence the mutual anisotropic effect of the aromatic rings.

Considering the polarity of the diastereoisomeric oxazolidinones[5] **6a** (Table 1), it is shown that the H4–H7 and H16–H20 signals of the more polar (3*S*,14*S*)-**6a** appear at lower frequency values than those of the less polar (3*R*,14*S*)-**6a** (Fig. 3), while the H8A signal for the less polar (3*R*,14*S*)-**6a** appears at lower frequency values than that of the more polar (3*S*,14*S*)-**6a**.

The assumption that aromatic moieties in (*S*)-oxazolidinyl and oxindolyl fragments influence each other, thus affecting their chemical shifts at H4–H7 and H16–H20 in **6a**–**e** is reinforced when considering the δ values for the aromatic hydrogen signals in phenyloxazolidinone **4** and oxindole derivatives **7** and **8**[2i,10] (Fig. 4). The chemical shifts for the aromatic hydrogens in these compounds are more similar to those of the less polar oxazolidinone (3*S*,14*R*)-**6a** diastereomer, which did not show the mutual aromatic ring anisotropic effect.

The observed $\Delta\delta^{RS}$ signs for both **6a** diastereomers could be accounted for by using the representation proposed in Figure 5, where the substituent arrangement around C3 and C14 in (3*S*,14*S*)-**6a** shows that the dominating conformation of the oxazolidinone should be that in which the orientation of the magnetic anisotropy imposed by both phenyl groups of the (*S*)-oxazolidinyl and oxindolyl moieties spends enough time to shield the H4–H7 and H16–H20 signals, whereas H8A is deshielded by the C11 carbonyl group (Fig. 5, **A**). In the (3*R*,14*S*)-**6a** diastereomer, the H4–H7, H16–H20, and H8A signals are not affected by both aromatic rings, nor by the C11 carbonyl group (Fig. 5, **B**). Therefore, the H4–H7 and H16–H20 signals will be more shielded in (3*S*,14*S*)-**6a** than in (3*R*,14*S*)-**6a**, while the H8A signal should be more shielded in (3*R*,14*S*)-**6a** than in (3*S*,14*S*)-**6a**.

It has been demonstrated that, in general, *N*-acyl oxazolidinones such as **9** are more stable in their *s-trans* conformation. The zero-point calculated energy difference of the *s-cis* and *s-trans* conformations ranged between 4.30 and 11.92 kcal/mol (Scheme 2).[11] Therefore structures (3*S*,14*S*)-**6a** (**A**) and (3*R*,14*S*)-**6a** (**B**) in Figure 6 should mainly adopt an *s-trans* array of the C9=O and C11=O carbonyl groups from which the remaining substituents at C8 and C14 protrude. This rigidity could stem from the oxazolidinone ring and from the dipole–dipole repulsion of the two C9=O and C11=O carbonyl groups.[5,12] Furthermore, it has been found that in *N*-acyloxazolidinones of type **9**, the barrier to rotation around the O=C–R^2 single bond is lower than that of the (R^2)O=C–N bond. Thus, the free rotation around the C8–C9=O bond generates three main conformers **I**–**III** for both diastereomers of **6a**. Conformer **I** should be the most populated in both diastereomers due to the lower steric effects between the oxindolyl and phenyloxazolidinyl rings. As shown in conformer **I** for (3*S*,14*S*)-**6a** (**A**) the mutual anisotropic shielding of both phenyl rings is present and consequently an upfield shift of the H4–H7 and H16–H20 signals should always occur. On the other side, in conformer **I** such an interaction was not observed for (3*R*,14*S*)-**6a** (**B**).

The aforementioned ^{1}H NMR configuration assignment methodology was extended to oxazolidinones with substituents other than a methyl group at the *N*1 and C3 positions, including the substrates shown in Table 2; the results confirm the applicability of the methodology. The $\Delta\delta^{RS}$ values obtained for oxazolidinones **6b**–**e** have the same sign for the H4–H7, H16–H20, and H8A signals and suggest that oxazolidinones **6b**–**e** adopt similar conformations

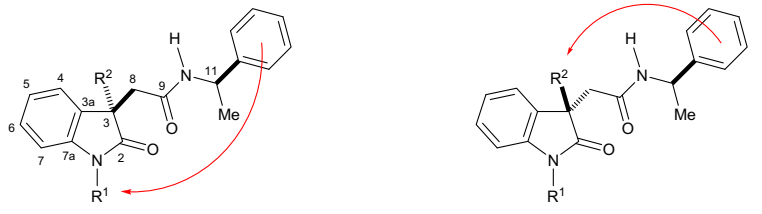

Figure 2.

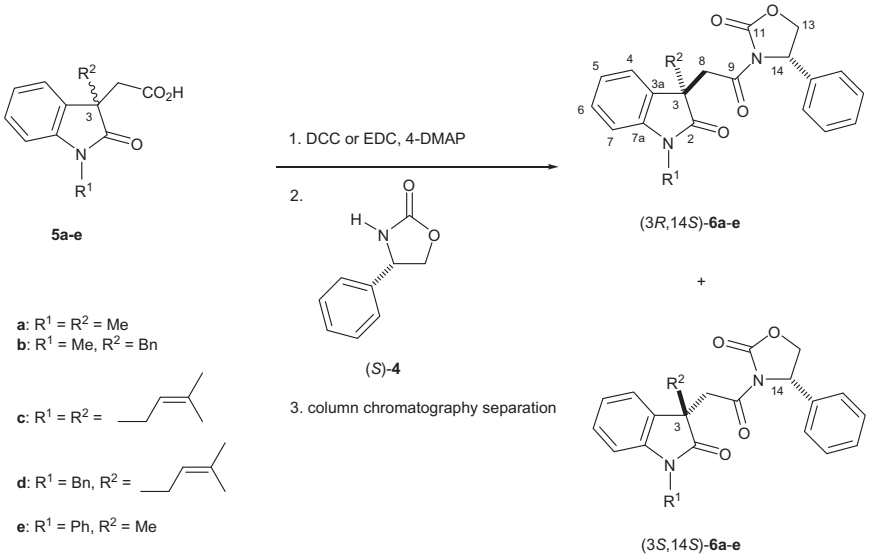

Scheme 1.

Table 1
R_f[a] values of diastereomeric oxazolidinones **6a**–**e**

Compound	(3*R*,14*S*)-Diastereomer R_f	(3*S*,14*S*)-Diastereomer R_f
6a	0.49	0.23
6b	0.74	0.53
6c	0.72	0.55
6d	0.56	0.28
6e	0.71	0.51

[a] Determined by TLC (Silica gel F_{254} coated aluminum sheets 0.25 mm thickness) using EtOAc/hexanes (1:1, v/v).

at the C8–(C9═O)–N10–C11═O fragment regardless of the substituents at the *N*1- and C3-positions.

Molecular modeling protocols with Monte Carlo searching[13] and geometry optimization using DFT calculations at the B3LYP/6-31G(d),[14] B3LYP/DGDZVP,[15] and B3PW91/DGDZVP2[16] levels of theory were applied to oxazolidinones (3*S*,14*S*)-**6a** and (3*R*,14*S*)-**6a** in order to find further evidence to explain the $\Delta\delta^{RS}$ values observed in Figure 6 and Table 2. The Monte Carlo search protocol using the MMFF94[17] molecular mechanics force field method, as implemented in the SPARTAN04[18] program, afforded 8 conformers for oxazolidinone (3*S*,14*S*)-**6a** (**6a*A*–*H***) and 9 conformers for (3*R*,14*S*)-**6a** (**6a*A*–*I***) within 4.1 and 7.6 kcal/mol gaps, respectively (Table 3). These structures were submitted to geometry optimization using DFT calculations at the B3LYP/6-31G(d) level of theory from which 6 conformers for oxazolidinone (3*S*,14*S*)-**6a** (**6a*A*–*C***, **6a*E*–*G***) and 7 conformers for oxazolidinone (3*R*,14*S*)-**6a** (**6a*A*–*E***, **6a*H*,*I***) accounted for 100% within 2.5 and 4.3 kcal/mol gaps, respectively. Further successive DFT geometry optimizations were carried out at the B3LYP/DGDZVP and B3PW91/DGDZVP2 levels of theory, respectively, as implemented in the GAUSSIAN 03W[19] program, giving 4 conformers for both (3*S*,14*S*)-**6a** (**6a*A***, **6a*C***, **6a*E***, **6a*G***) and (3*R*,14*S*)-**6a** (**6a*A*–*D***) oxazolidinones, which are shown in Figures 7 and 8, respectively, while their relative energies are shown in Table 3. The population of each conformational species was estimated using the thermochemical parameters in the conformational equilibrium using the $\Delta G = \Delta H - T\Delta S$ and $\Delta G = -RT\ln K$ equations (Table 3).[3] For conformational equilibria of both (3*S*,14*S*)-**6a** and (3*R*,14*S*)-**6a** diastereomers, equations $K_{1,2} = n_2/n_1$, $K_{2,3} = n_3/n_2$, $K_{3,4} = n_4/n_3$, and $n_1 + n_2 + n_3 + n_4 = 1$ were used, where $K_{i,j}$ stands for the equilibria constants and n_i stands for the molar fraction. It is worth noting that the *s-trans* arrays of the C9═O and C11═O carbonyl groups were always detected as the most stable conformations, irrespective of the diastereomeric oxazolidinone **6a** studied. With these results, it becomes evident that the free rotation around the C8–C9═O single bond (Fig. 6) is the dominating process in both diastereomers. Conformers (3*S*,14*S*)-**6a*A***, **6a*C***, **6a*E.*** and **6a*G*** (Fig. 7) and (3*R*,14*S*)-**6a*A*–*D*** (Fig. 8) are depicted as the most populated in the conformational equilibria for oxazolidinones **6a**. It is interesting to note that for oxazolidinone (3*S*,14*S*)-**6a**, the global minimum structure **6a*A*** (81.4%) has the phenyl rings pointing toward each other, in exact coincidence with conformer **I** presented in Figure 6, trace **A**. Regarding oxazolidinone (3*R*,14*S*)-**6a**, three of the most abundant conformers (**6a*A*, 6a*B*** and **6a*D*** 94.7%) show both aromatic rings far from each other, thus eliminating the mutual anisotropic effect. The global minimum (3*S*,14*S*)-**6a*A*** and (3*R*,14*S*)-**6a*B*** conformers corresponded very well with those predicted in Figure 6 and with the experimental results. Thus, computational results reinforce the assignment of the absolute configuration in (3*S*,14*S*)-**6a** and (3*R*,14*S*)-**6a**.

The reliability of our methodology for the absolute configuration assignment of oxazolidinones **6a**–**e** by ^{1}H NMR was supported by X-ray diffraction analysis of oxazolidinones (3*S*,14*S*)-**6a**, (3*S*,14*S*)-**6d**, (3*R*,14*S*)-**6e** and (3*S*,14*S*)-**6e**, whose structures are shown in Figure 9 (Table 4). These results validate the assignment of the absolute configuration of oxazolidinones **6a**–**e** by ^{1}H NMR using (*S*)-phenyloxazolidinone **4** as a CDA.

Similarly, when (*R*)-phenyloxazolidinone (*R*)-**4** was used as a CDA to resolve the (±)-**5a** oxazolidinone mixture, (3*S*,14*R*)-**6a** and (3*R*,14*R*)-**6a** were obtained in a 90% yield (Scheme 3). As expected, the ^{1}H NMR spectra showed preferential shielding of the H4–H7 and H16–H20 signals and deshielding of the H8A signal for diastereomer (3*R*,14*R*)-**6a** (Table 2), whereas preferential shielding of the H8A signal and deshielding of H4–H7 and H16–H20 signals were observed for oxazolidinone (3*S*,14*R*)-**6a** (Table 2). Oxazolidinone (3*R*,14*R*)-**6a** gave crystals suitable for X-ray diffraction analysis and the corresponding structure is shown in Figure 9 (Table 4).

With this result in hand, we were able to assign the absolute configuration of the reported oxazolidinones (3*R*,14*R*)-**10** and (3*S*,14*R*)-**10**, which have been used as intermediates in the total synthesis of (−)- and (+)-debromoflustramine A **11**, respectively (Scheme 4).[20] The relative configuration in (3*R*,14*R*)-**10** and (3*S*,14*R*)-**10** was tentatively assigned by their transformation to

Table 2
Significant $\Delta\delta^{RS}$ values for (3*R*,14*S*)-**6a**–**e**–(3*S*,14*S*)-**6a**–**e** and (3*R*,14*R*)-**10**–(3*S*,14*R*)-**10**[20] and $\Delta\delta^{SR}$ values for (3*S*,14*R*)-**6a**–(3*R*,14*R*)-**6a**[a]

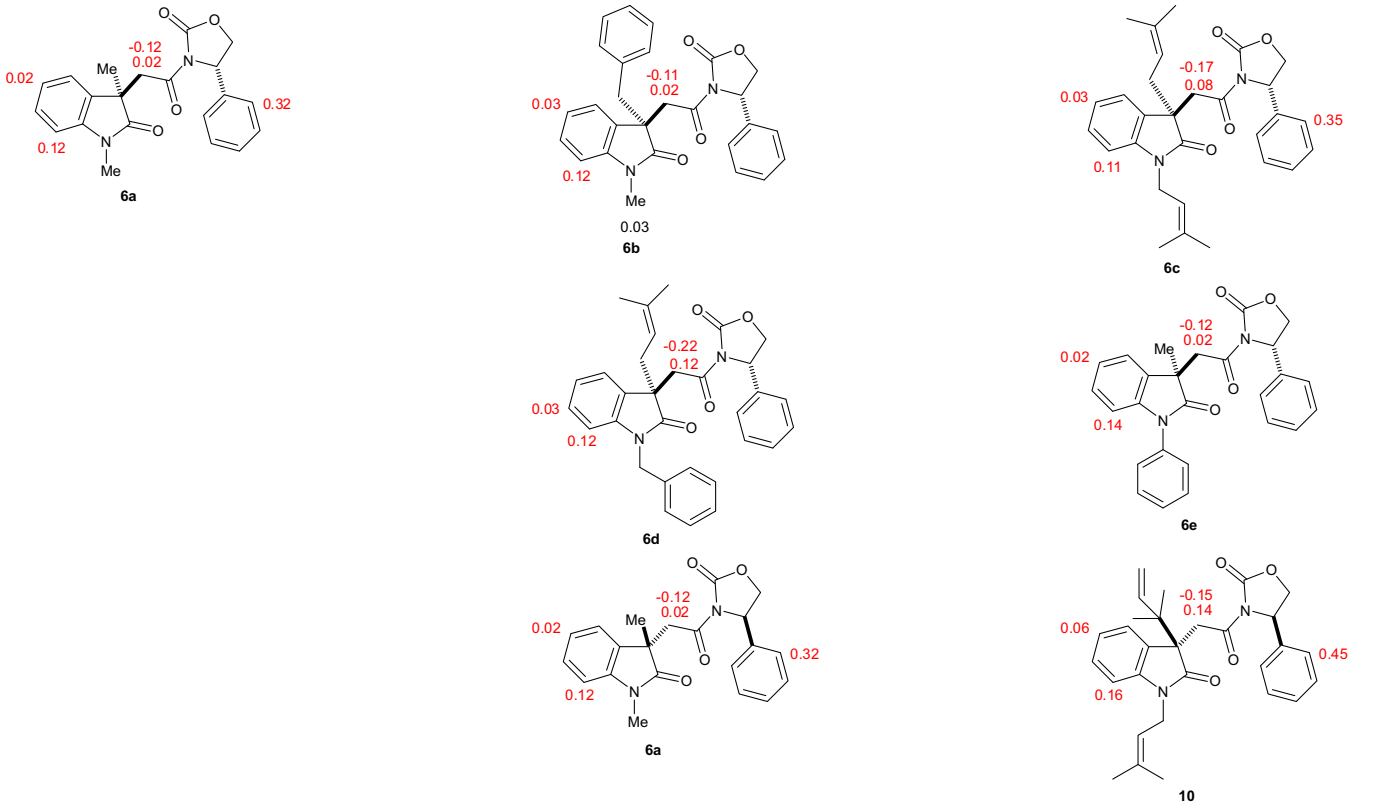

[a] $\Delta\delta^{RS}$ Values ($\delta_R - \delta_S$) were obtained by subtracting the ^{1}H chemical shifts of (3*S*)-oxyndolyl–(14*S*)-oxazolidinone from those of (3*R*)-oxyndolyl–(14*S*)-oxazolidinone **A** while $\Delta\delta^{SR}$ values ($\delta_S - \delta_R$) were obtained by subtracting the ^{1}H chemical shifts of (3*R*)-oxyndolyl–(14*R*)-oxazolidinone from those of (3*S*)-oxyndolyl-(14*R*)-oxazolidinone **B**.[3,9]

(−)-**11** and (+)-**11**, respectively. The stereochemistry of (−)-**11** was elucidated by comparing specific rotations of known pyrrolo[2,3-*b*]indole compounds, for example, (−)-flustramines and (−)-physostigmine, although this is not necessarily a completely safe comparison methodology as evidenced recently.[21] According to the aforementioned methodology, for the (3*R*,14*R*)-**10** diastereomer, the H4–H7 and H16–H20 signals are deshielded whereas the H8A signal is shielded.[20] On the contrary, in diastereomer (3*S*,14*R*)-**10** the H4–H7 and H16–H20 signals are shielded while H8A is deshielded. Thus, considering our NMR methodology, the absolute configurations of the reported oxazolidinones (3*R*,14*R*)-**10** and (3*S*,14*R*)-**10** are those shown in Scheme 4. It is worth noting that although the absolute configuration at C3 in (3*R*,14*R*)-**6a** and (3*S*,14*R*)-**10** are opposite, due to proper application of the Cahn-Ingold-Prelog sequence rule,[22] the spatial relationship of the methyl -methyl and -dimethylallyl groups with respect to the phenyl ring at C14 is the same in these compounds, allowing mutual anisotropic effect of both aryl rings.

To further substantiate our assignments, the absolute configurations of (3*S*,14*S*)-**6a** and (3*R*,14*S*)-**6a** were independently determined using vibrational circular dichroism (VCD) spectroscopy. Thus, for both diastereomers the vibrational frequencies and IR and VCD intensities were calculated at the B3PW91/DGDZVP2[16] level of theory. The calculations involve the generation of weighted-averaged vibrational plots including conformers **6a*A***, **6a*C***, **6a*E***, and **6a*G*** for (3*S*,14*S*)-**6a** oxazolidinone and conformers **6a*A*–*D*** for diastereomer (3*R*,14*S*)-**6a**. The VCD frequencies of these major conformers were calculated and Boltzmann-averaged to generate the calculated spectrum which was plotted using Lorentzian bandshapes and bandwidths of 6 cm^{-1}. The calculated IR and VCD spectra of (3*S*,14*S*)-**6a** and (3*R*,14*S*)-**6a** showed good agreement with those obtained experimentally (Figs. 10 and 11). In order to avoid bias when assessing the degree of agreement between computed and experimental spectra by visual inspection, quantitative evaluation of this concordance was achieved by applying a recently developed confidence level algorithm (BioTools Co., Jupiter, FL 33458, USA) which calculates the integrated overlap of the experimental and theoretical data as a function of a relative shift.[23] Application of this procedure allowed us to obtain the anharmonicity factor (*anH* = 0.975), and the VCD spectral similarity for the correct (S_E = 75.4%) and the incorrect enantiomer (S_{-E} = 20.4%) with a 100% confidence level for the absolute configuration determination of (3*S*,14*S*)-**6a** oxazolidinone, while for the (3*R*,14*S*)-**6a** diastereomer *anH* = 0.972, S_E = 83.4%, and S_{-E} = 13.4% with a 100% confidence level for the absolute configuration determination were obtained. These results undoubtedly allow us to conclude that ^{1}H NMR is a reliable method for the absolute configuration assignment of oxindoles such as (3*S*,14*S*)-**6a** and (3*R*,14*S*)-**6a**.

3. Conclusions

We have demonstrated that the absolute configuration assignment of 2-(2-oxo-3-indolyl)acetic acid derivatives **5** could be achieved by its derivatization with either commercially available

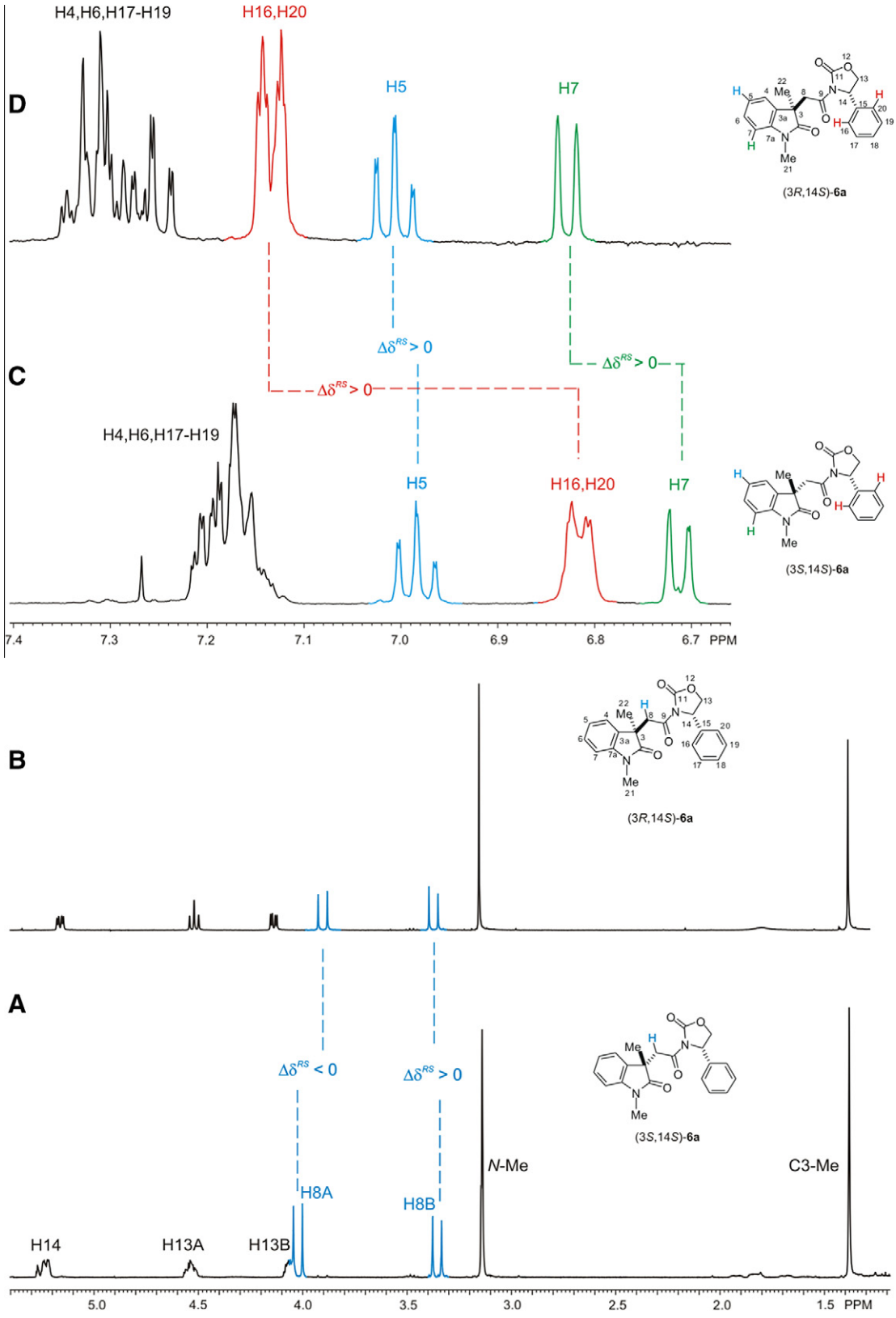

Figure 3.

enantiomer of 4-phenyl-2-oxazolidinone (*S*)-**4** or (*R*)-**4** followed by ^{1}H NMR analysis of the corresponding oxazolidinones **6**. A general assumption could be made for the configuration assignment as follows: (3*S*,14*S*)- or (3*R*,14*R*)-stereoisomers of oxazolidinones of type **6** will present the H4–H7 and H16–H20 signals at lower frequency values ($+\Delta\delta^{RS}$ or $+\Delta\delta^{SR}$) and the H8A signal at a higher frequency value ($-\Delta\delta^{RS}$ or $-\Delta\delta^{SR}$) when compared to their corresponding (3*R*,14*S*)- and (3*S*,14*R*)-diastereomers. The results were independently confirmed by X-ray diffraction analysis, VCD measurements, and calculations.

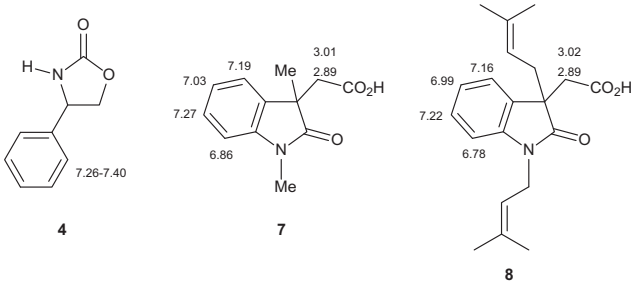

Figure 4. Aromatic ^{1}H chemical shifts (in ppm) for **4**, **7** and **8** in $CDCl_3$.

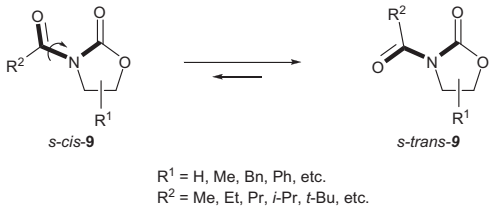

Scheme 2.

4. Experimental

4.1. General experimental procedures

Melting points were determined on a Büchi B-540 apparatus. IR spectra were recorded on a Perkin–Elmer 2000 FT-IR spectrophotometer. The 400 and 100 MHz ^{1}H and ^{13}C NMR spectra were obtained on JEOL Eclipse +400 and on Varian VNMRS 400 spectrometers, while the 300 and 75 MHz ^{1}H and ^{13}C NMR spectra were obtained on a Varian Mercury-300 spectrometer using $CDCl_3$ as solvent and TMS as the internal reference. For complete assignments gHMQC, gHSQC, and gHMBC spectra were measured. Data are reported as follows: chemical shift in ppm from TMS, integration, multiplicity (s = singlet, d = doublet, t = triplet, sp = septet, AB = AB system, m = multiplet, br = broad), coupling constant (Hz), and assignment. GC/MS analyses were conducted on a Varian CP 3800 GC equipped with a Varian Saturn 2000 selective mass detector and a 30 m, 0.25 mm i.d., 0.25 mm CP-SIL capillary column, using helium as a carrier gas (1 mL/min), programed from 70 °C to 250 °C at a rate of 30 °C/min, with the injector temperature at 200 °C. MS were obtained in the electron impact (EI) mode at an ionizing voltage of 70 eV on a Hewlett Packard 5989-A spectrometer. High-resolution (HR) mass spectra were measured on a JEOL JMS-SX 102A mass spectrometer at the Instituto de Química, UNAM-México. Optical rotation measurements were performed on a Perkin–Elmer 341 polarimeter. Analytical thin-layer chromatography (TLC) was done on silica gel F_{254} coated aluminum sheets (0.25 mm thickness) with a fluorescent indicator. Visualization was accomplished with UV light (254 nm). Flash chromatography was done using Silica Gel 60 (230–400 mesh) from Aldrich.

4.2. General procedure for the preparation of diastereomeric amides 6a–e

A solution of the appropriate acids **5a**–**d** (3.20 mmol), **5e** (0.36 mmol), (*S*)-(+)-4-phenyl-2-oxazolidinone (*S*)-**4** (0.52 g, 3.2 mmol for **5a**–**d** and 0.06 g, 0.36 mmol for **5e**), 4-DMAP (0.17 g, 1.4 mmol for **5a**–**d** and 0.017 g, 0.14 mmol for **5e**) and DCC (0.76 g, 3.68 mmol) in CH_2Cl_2 (20 mL) for **5a**–**d** or EDC·HCl (0.08 g, 0.43 mmol) in toluene (20 mL) for **5e** was stirred for 24 h at rt and then at reflux for 2.5 h for **5a**–**d** and at reflux for 2 h for **5e**. After cooling to room temperature, the reaction mixture was filtered and the solvent evaporated. The residue **6e** was diluted with CH_2Cl_2 (40 mL) and washed with water (2 × 10 mL), an aqueous solution of HCl (1 M, 2 × 10 mL) and a saturated aqueous solution of $NaHCO_3$ (2 × 20 mL), dried over Na_2SO_4, filtered, and evaporated. The residues **6a**–**e** were purified by flash column chromatography on silica gel with EtOAc/hexanes 2:3 for **6a** and **6b**, with EtOAc/hexanes 1:2 for **6c**–**6d** and with EtOAc/hexanes 2:1 for **6e**.

4.2.1. (*S*)-3-(2-((*R*)-1,3-Dimethyl-2-oxoindolin-3-yl)acetyl)-4-phenyloxazolidin-2-one (3*R*,14*S*)-6a

Prepared from **5a** as a white solid (0.23 g, 45%), mp: 197–198 °C (MeOH). $[\alpha]_D^{20} = +118.7$ (*c* 0.81, $CHCl_3$). ^{1}H NMR (400 MHz, $CDCl_3$): δ 7.35–7.27 (3H, m, H17–H19), 7.26 (1H, td, *J* = 7.7, 1.1 Hz, H6), 7.13 (3H, m, H4, H16, H20), 7.00 (1H, td, *J* = 7.6, 1.0 Hz, H5), 6.83 (1H, d, *J* = 7.7 Hz, H7), 5.16 (1H, dd, *J* = 8.8, 3.3 Hz, H14), 4.52 (1H, t, *J* = 8.8 Hz, H13A), 4.14 (1H, dd, *J* = 8.8, 3.3 Hz, H13B), 3.90 and 3.37 (2H, AB, *J* = 17.4 Hz, H8), 3.16 (3H, s, H21), 1.39 (3H, s, H22);

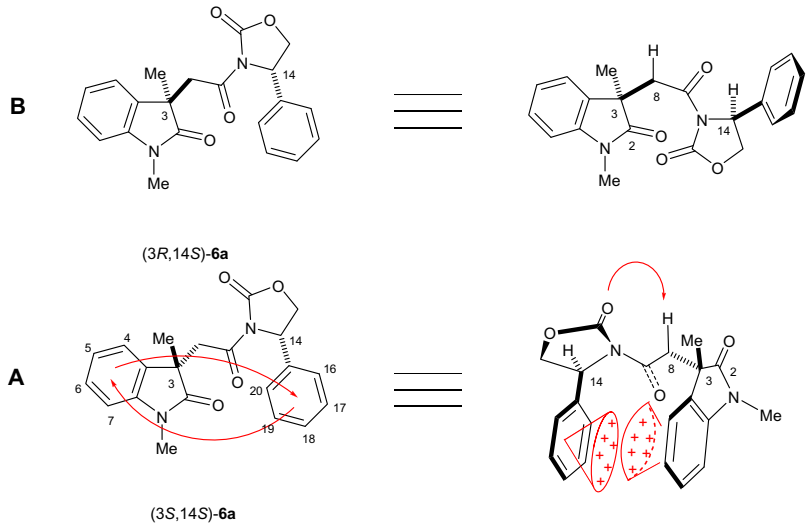

Figure 5.

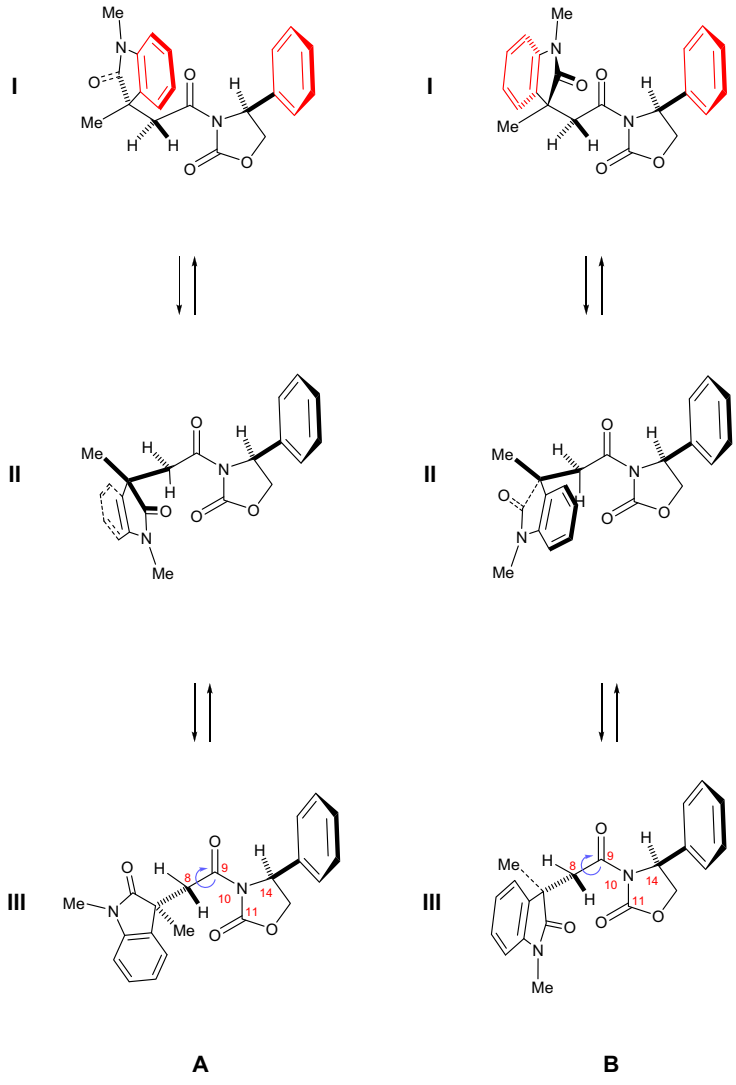

Figure 6. Preferred conformations of (3*S*,14*S*)-**6a** (**A**) and (3*R*,14*S*)-**6a** (**B**) phenyloxazolidinones.

^{13}C NMR (100 MHz, $CDCl_3$): δ 179.6 (C2), 168.7 (C9), 153.8 (C11), 143.6 (C7a), 138.4 (C15), 133.2 (C3a), 129.1 (2C, C17, C19), 128.5 (C18), 127.9 (C6), 125.5 (2C, C16, C20), 122.1 (C5), 121.7 (C4), 108.1 (C7), 70.0 (C13), 57.1 (C14), 45.4 (C3), 42.0 (C8), 26.3 (C21), 24.6 (C22); IR (KBr) ν_{max} 3053, 3034, 2972, 2926, 1787, 1719, 1613, 1495, 1472, 1454 cm^{-1}; EIMS *m*/*z* (relative intensity) 364 ([M]$^+$, 100), 186 (30), 174 (48), 160 (46); FABHRMS *m*/*z* calcd for $C_{21}H_{20}N_2O_4$ ([M]$^+$): 364.1423, found: 364.1416.

4.2.2. (*S*)-3-(2-((*S*)-1,3-Dimethyl-2-oxoindolin-3-yl)acetyl)-4-phenyloxazolidin-2-one (3*S*,14*S*)-6a

Prepared from **5a** as colorless crystals (0.23 g, 45%), mp: 172–173 °C (CH_2Cl_2). $[\alpha]_D^{20} = +184.3$ (*c* 1.08, $CHCl_3$). ^{1}H NMR (300 MHz, $CDCl_3$): δ 7.22–7.10 (5H, m, H4, H6, H17–H19), 6.98 (1H, td, *J* = 7.5, 0.8 Hz, H5), 6.81 (2H, m, H16, H20), 6.71 (1H, dd, *J* = 8.2, 0.7 Hz, H7), 5.22 (1H, br dd, *J* = 8.5, 3.5 Hz, H14), 4.52 (1H, br t, *J* = 8.7 Hz, H13A), 4.05 (1H, m, H13B), 4.02 and 3.35 (2H, AB, *J* = 17.1 Hz, H8), 3.13 (3H, s, H21), 1.38 (3H, s, H22); ^{13}C NMR (75 MHz, $CDCl_3$): δ 179.9 (C2), 168.6 (C9), 153.6 (C11), 143.5 (C7a), 138.2 (C15), 132.8 (C3a), 128.8 (2C, C17, C19), 128.0 (C18), 127.9 (C6), 125.0 (2C, C16, C20), 122.0 (C5), 121.8 (C4), 108.1 (C7), 69.9 (C13), 57.0 (C14), 45.6 (C3), 41.7 (C8), 26.2 (C21), 24.6 (C22); IR (film) ν_{max} 3057, 3009, 2969, 2928, 1779, 1710, 1614, 1495, 1472, 1453 cm^{-1}; EIMS *m*/*z* (relative intensity) 364 ([M]$^+$, 100), 186 (22), 174 (18), 160 (16); FABHRMS *m*/*z* calcd for $C_{21}H_{20}N_2O_4$ ([M]$^+$): 364.1423, found: 364.1415.

4.2.3. (*S*)-3-(2-((*R*)-1,3-Dimethyl-2-oxoindolin-3-yl)acetyl)-4-phenyloxazolidin-2-one (3*S*,14*R*)-6a

Prepared from **5a** and (*R*)-(−)-4-phenyl-2-oxazolidinone (*R*)-**4** as colorless crystals (0.23 g, 45%), mp: 198–199 °C (MeOH). $[\alpha]_D^{20} = -120.0$ (*c* 0.69, $CHCl_3$). Spectroscopic data are identical with those of its (3*R*,14*S*)-**6a** enantiomer.

4.2.4. (*R*)-3-(2-((*R*)-1,3-Dimethyl-2-oxoindolin-3-yl)acetyl)-4-phenyloxazolidin-2-one (3*R*,14*R*)-6a

Prepared from **5a** and (*R*)-(−)-4-phenyl-2-oxazolidinone (*R*)-**4** as colorless crystals (0.23 g, 45%), mp: 172–173 °C (CH_2Cl_2). $[\alpha]_D^{20} = -183.5$ (*c* 0.68, $CHCl_3$). Spectroscopic data are identical with those of its (3*S*,14*S*)-**6a** enantiomer.

4.2.5. (*S*)-3-(2-((*R*)-3-Benzyl-1-methyl-2-oxoindolin-3-yl)acetyl)-4-phenyloxazolidin-2-one (3*R*,14*S*)-6b

Prepared from **5b** as white crystals (0.26 g, 42%), mp: 190–191 °C (CH_2Cl_2/MeOH). $[\alpha]_D^{20} = +138.9$ (*c* 1.82, $CHCl_3$). ^{1}H NMR (300 MHz, $CDCl_3$): δ 7.37–7.00 (10H, m, H4, H6, H16–H20, H25–H27), 6.97 (1H, td, *J* = 7.4, 1.0 Hz, H5), 6.78

Table 3
Thermochemical analysis for oxazolidinones (3*S*,14*S*)-**6a** and (3*R*,14*S*)-**6a**

Conformer	ΔE_{MMFF}[a]	%MMFF[b]	ΔE_{DFT}[c]	%DFT[d]	ΔG_{OPT}[e]	%OPT[f]	ΔG_{OPT}[g]	%OPT[h]
*(3S,14S)-**6a***								
6a*A*	0	57.0	0.79	10.8	0	74.3	0	81.4
6a*B*	0.46	26.3	0	41.1	—	—	—	—
6a*C*	1.00	10.5	0.20	29.5	1.40	6.6	2.20	1.8
6a*D*	1.52	4.4	—	—	—	—	—	—
6a*E*	2.40	1.0	0.54	16.5	0.76	18.9	0.91	16.7
6a*F*	3.01	0.4	1.98	1.5	—	—	—	—
6a*G*	3.04	0.3	2.45	0.7	3.39	0.2	4.15	0.1
6a*H*	4.09	0.1	—	—	—	—	—	—
*(3R,14S)-**6a***								
6a*A*	0	96.3321	0	63.77	0.48	23.1	1.04	12.4
6a*B*	2.50	1.4079	0.76	17.54	0	48.4	0	67.0
6a*C*	2.88	0.7427	1.43	5.71	0.75	13.6	1.50	5.3
6a*D*	2.90	0.7207	1.00	11.79	0.76	13.6	0.87	15.3
6a*E*	3.31	0.3639	2.43	1.05	2.24	1.1	—	—
6a*F*	3.39	0.3160	—	—	—	—	—	—
6a*G*	4.26	0.0724	—	—	—	—	—	—
6a*H*	4.56	0.0441	4.27	0.05	—	—	—	—
6a*I*	7.59	0.0003	3.88	0.09	3.66	0.1	—	—

[a] Molecular mechanics energies relative to (3*S*,14*S*)-**6a*A*** with $E_{MMFF} = -16.613$ kcal/mol or relative to (3*R*,14*S*)-**6a*A*** with $E_{MMFF} = -17.878$ kcal/mol.
[b] Population in % calculated from the MMFF energies according to $\Delta E_{MMFF} \approx -RT\ln K$.
[c] Single point B3LYP/6-31G(d) energies relative to (3*S*,14*S*)-**6a*B*** with $E_{6\text{-}31G(d)} \approx -RT\ln K = -767280.695$ kcal/mol or relative to (3*R*,14*S*)-**6a*A*** with $E_{6\text{-}31G(d)} \approx -RT\ln K = -767281.432$ kcal/mol.
[d] Population in % calculated from B3LYP/6-31G(d) energies according to $\Delta E_{6\text{-}31G(d)} \approx -RT\ln K$.
[e] Gibbs free energies relative to (3*S*,14*S*)-**6a*A*** with $G_{B3LYP/DGDZVP} = -767160.601$ kcal/mol or relative to (3*R*,14*S*)-**6a*B*** with $G_{B3LYP/DGDZVP} = -767160.701$ kcal/mol.
[f] Population in % calculated from B3LYP/DGDZVP energies according to $\Delta G = -RT\ln K$.
[g] Gibbs free energies relative to (3*S*,14*S*)-**6a*A*** with $G_{B3PW91/DGDZVP2} = -766949.457$ kcal/mol or relative to (3*R*,14*S*)-**6a*B*** with $G_{B3PW91/DGDZVP2} = -766949.517$ kcal/mol.
[h] Population in % calculated from B3PW91/DGDZVP2 energies according to $\Delta G = -RT\ln K$.

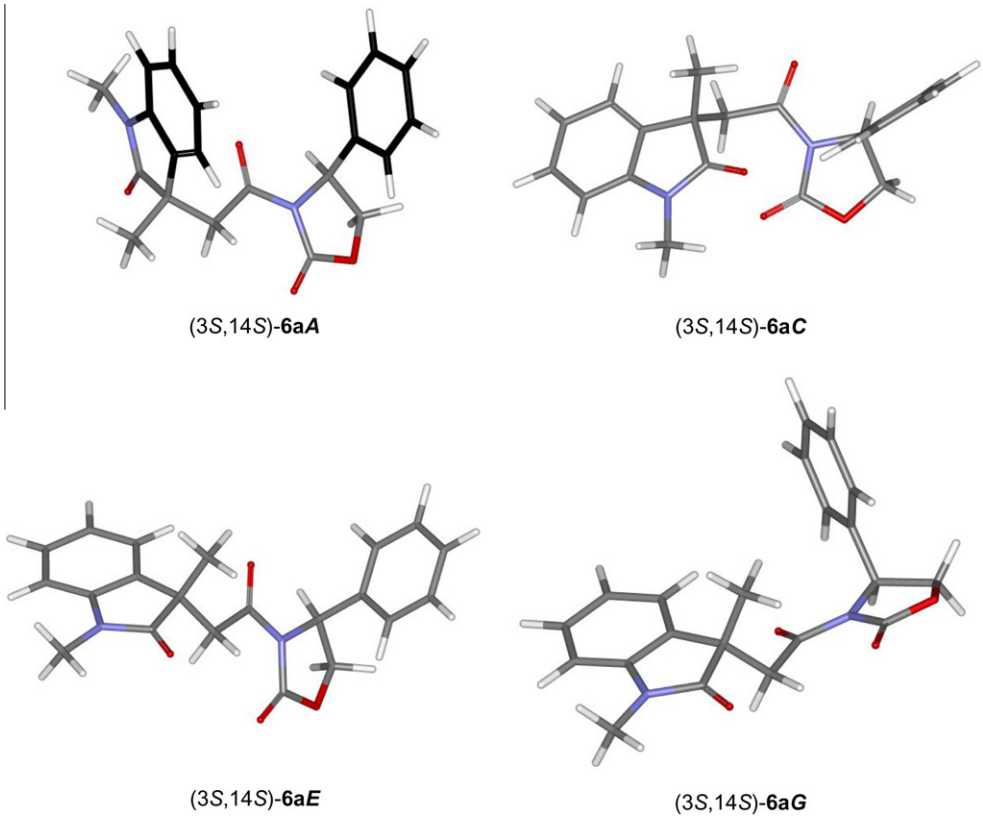

Figure 7. Optimized geometries for (3*S*,14*S*)-**6a*A***, **6a*C***, **6a*E*** and **6a*G*** conformers using DFT calculations at the B3PW91/DGDZVP2 level of theory.

(2H, dd, $J = 7.8$, 1.7 Hz, H24, H28), 6.54 (1H, br d, $J = 7.6$ Hz, H7), 5.18 (1H, dd, $J = 8.6$, 3.5 Hz, H14), 4.53 (1H, dd, $J = 8.7$ Hz, H13A), 4.15 (1H, dd, $J = 8.8$, 3.5 Hz, H13B), 4.03 and 3.53 (2H, AB, $J = 17.4$ Hz, H8), 3.07 (2H, s, H22), 2.87 (3H, s, H21); ^{13}C NMR (75 MHz, $CDCl_3$): δ 178.2 (C2), 168.6 (C9), 153.9 (C11), 144.2 (C7a), 138.4 (C15), 134.7 (C23), 130.4 (C3a), 130.0 (2C, C24,

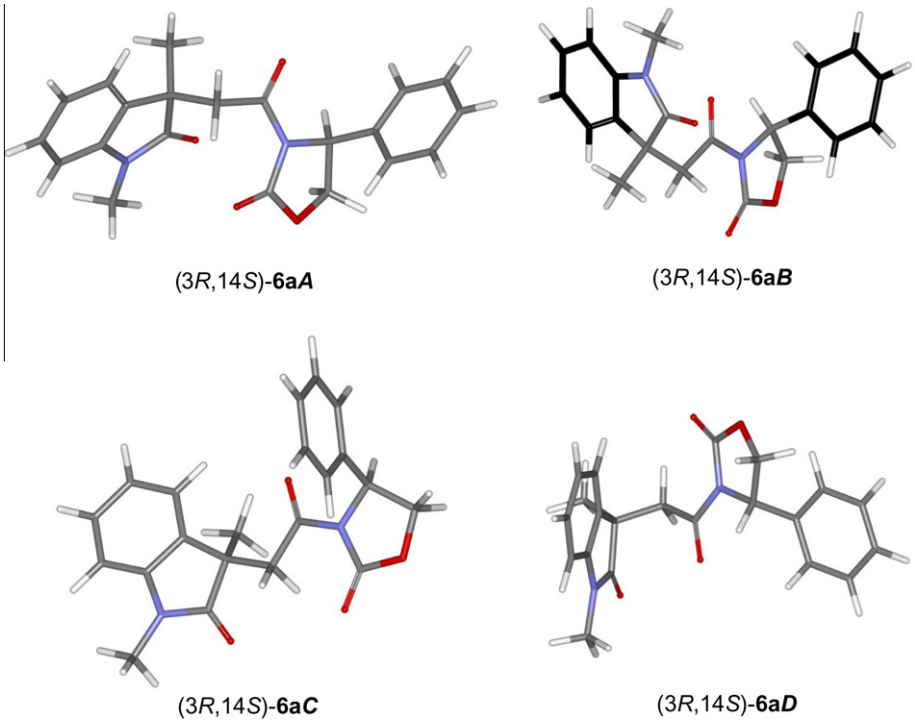

Figure 8. Optimized geometries for (3*R*,14S)-**6a*A*–*D*** conformers using DFT calculations at the B3PW91/DGDZVP2 level of theory.

C28), 129.1 (C17, C19), 128.6 (C18), 128.1 (C6), 127.4 (2C, C25, C27), 126.6 (C26), 125.5 (2C, C16, C20), 122.7 (C4), 121.7 (C5), 107.8 (C7), 70.1 (C13), 57.1 (C14), 51.2 (C3), 44.1 (C22), 41.0 (C8), 25.9 (C21); IR (film) ν_{max} 3060, 3031, 2921, 1780, 1708, 1613, 1495, 1471, 1455 cm^{-1}; EIMS *m*/*z* (relative intensity) 440 ([M]$^+$, 13), 186 (100), 91 (10); FABHRMS *m*/*z* calcd for $C_{27}H_{24}N_2O_4$ ([M]$^+$): 440.1736, found: 440.1744.

4.2.6. (*S*)-3-(2-((*S*)-3-Benzyl-1-methyl-2-oxoindolin-3-yl)-acetyl)-4-phenyloxazolidin-2-one (3*S*,14*S*)-6b

Prepared from **5b** as white crystals (0.26 g, 42%), mp: 168–169 °C (EtOAc/hexane). $[\alpha]_D^{20} = +183.7$ (*c* 1.26, $CHCl_3$). ^{1}H NMR (300 MHz, $CDCl_3$): δ 7.15–7.00 (8H, m, H4, H6, H17–H19, H25–H27), 6.94 (1H, br t, *J* = 7.4 Hz, H5), 6.81–6.74 (4H, m, H16, H20, H24, H28), 6.42 (1H, br d, *J* = 7.6 Hz, H7), 5.20 (1H, br dd, *J* = 8.4, 3.3 Hz, H14), 4.50 (1H, br t, *J* = 8.0 Hz, H13A), 4.14 and 3.51 (2H, AB, *J* = 17.2 Hz, H8), 4.03 (1H, br dd, *J* = 8.8, 3.5 Hz, H13B), 3.06 (2H, s, H22), 2.84 (3H, s, H21); ^{13}C NMR (75 MHz, $CDCl_3$): δ 178.4 (C2), 168.5 (C9), 153.7 (C11), 144.0 (C7a), 138.1 (C15), 134.6 (C23), 130.0 (C3a), 129.9 (2C, C24, C28) 128.7 (2C, C17, C19), 127.9 (2C, C6, C18), 127.3 (2C, C25, C27), 126.5 (C26), 124.9 (C16, C20), 122.6 (C4), 121.5 (C5), 107.7 (C7), 69.9 (C13), 57.0 (C14), 51.3 (C3), 44.2 (C22), 40.8 (C8), 25.8 (C21); IR (film) ν_{max} 3060, 3030, 2918, 1780, 1709, 1614, 1495, 1471, 1455 cm^{-1}; EIMS *m*/*z* (relative intensity) 440 ([M]$^+$, 13), 186 (100), 91 (10); FABHRMS *m*/*z* calcd for $C_{27}H_{24}N_2O_4$ ([M]$^+$): 440.1736, found: 440.1737.

4.2.7. (*S*)-3-(2-((*R*)-1,3-Bis(3-methylbut-2-enyl)-2-oxoindolin-3-yl)acetyl)-4-phenyloxazolidin-2-one (3*R*,14*S*)-6c

Prepared from **5c** as a white solid (0.28 g, 42%), mp: 122–123 °C (Et_2O/hexane). $[\alpha]_D^{20} = +90.0$ (*c* 1.34, $CHCl_3$). ^{1}H NMR (400 MHz, $CDCl_3$): δ 7.35–7.25 (3H, m, H17–H19), 7.20 (1H, br t, *J* = 7.7 Hz, H6), 7.14 (2H, br d, *J* = 8.0 Hz, H16, H20), 7.11 (1H, dd, *J* = 7.3, 0.7 Hz, H4), 6.96 (1H, t, *J* = 7.5, H5), 6.74 (1H, br d, *J* = 7.7 Hz, H7), 5.15 (1H, dd, *J* = 8.6, 3.5 Hz, H14), 5.02 (1H, tm, *J* = 6.6 Hz, H22), 4.81 (1H, tm, *J* = 7.7 Hz, H27), 4.51 (1H, br t, *J* = 8.8 Hz, H13A), 4.33 (1H, dd, *J* = 15.8, 6.6 Hz, H21A), 4.18–4.10 (2H, m, H13B, H21B), 3.93 and 3.40 (2H, AB, *J* = 17.6 Hz, H8), 2.49 (1H, dd, *J* = 13.6, 7.4 Hz, H26A), 2.44 (1H, dd, *J* = 13.7, 7.5 Hz, H26B), 1.74 (3H, s, H24), 1.65 (3H, s, H25), 1.57 (3H, s, H29), 1.47 (3H, s, H30); ^{13}C NMR (100 MHz, $CDCl_3$): δ 178.4 (C2), 168.7 (C9), 153.8 (C11), 143.5 (C7a), 138.5 (C15), 136.1 (C28), 135.7 (C23), 131.6 (C3a), 128.5 (2C, C17, C19) 127.7 (C18), 127.7 (C6), 125.6 (2C, C16, C20), 122.2 (C4), 121.6 (C5), 118.8 (C22), 116.9 (C27), 108.3 (C7), 70.0 (C13), 57.1 (C14), 49.6 (C3), 40.8 (C8), 37.9 (C21), 36.7 (C26), 25.8 (C29), 25.8 (C25), 18.0 (C24), 17.9 (C30); IR (KBr) ν_{max} 3036, 2965, 2919, 2855, 1793, 1724, 1611, 1489, 1467, 1436 cm^{-1}; EIMS *m*/*z* (relative intensity) 472 ([M]$^+$, 7), 404 (100), 267 (57), 242 (77), 215 (32), 185 (54), 172 (34), 158 (24), 145 (19), 69 (22), 41 (34); FABHRMS *m*/*z* calcd for $C_{29}H_{32}N_2O_4$ (M$^+$): 472.2362, found: 472.2361.

4.2.8. (*S*)-3-(2-((*S*)-1,3-Bis(3-methylbut-2-enyl)-2-oxoindolin-3-yl)acetyl)-4-phenyloxazolidin-2-one (3*S*,14*S*)-6c

Prepared from **5c** as a colorless oil (0.28 g, 42%). $[\alpha]_D^{20} = +91.0$ (*c* 1.01, $CHCl_3$). ^{1}H NMR (300 MHz, $CDCl_3$): δ 7.18 (1H, ddd, *J* = 7.3, 1.2, 0.5 Hz, H4), 7.17–7.10 (4H, m, H6, H17–H19), 6.93 (1H, td, *J* = 7.5, 1.0 Hz, H5), 6.79 (2H, m, H16, H20), 6.63 (1H, ddd, *J* = 7.7, 1.0, 0.5 Hz, H7), 5.23 (1H, dd, *J* = 8.6, 3.6 Hz, H14), 4.97 (1H, tsp, *J* = 6.5, 1.4 Hz, H22), 4.82 (1H, tsp, *J* = 7.6, 1.4 Hz, H27), 4.55 (1H, dd, *J* = 8.7 Hz, H13A), 4.38 (1H, br dd, *J* = 15.8, 6.2 Hz, H21A), 4.10 (1H, br dd, *J* = 15.5, 6.3 Hz, H21B), 4.07 (1H, dd, *J* = 8.4, 4.1 Hz, H13B), 4.10 and 3.32 (2H, AB, *J* = 16.9 Hz, H8), 2.50 (1H, dd, *J* = 13.7, 7.3 Hz, H26A), 2.47 (1H, dd, *J* = 13.7, 7.7 Hz, H26B), 1.76 (3H, d, *J* = 0.9 Hz, H24), 1.65 (3H, d, *J* = 0.9 Hz, H25), 1.56 (3H, d, *J* = 1.0 Hz, H29), 1.46 (3H, d, *J* = 1.2 Hz, H30); ^{13}C NMR (75 MHz, $CDCl_3$): δ 178.6 (C2), 168.7 (C9), 153.7 (C11), 143.5 (C7a), 138.3 (C15), 136.0 (C28), 135.4 (C23), 131.0 (C3a), 128.8 (2C, C17, C19) 127.9 (C18), 127.7 (C6), 125.0 (2C, C16, C20), 122.5 (C4), 121.6 (C5), 119.0 (C22), 116.9 (C27), 108.5 (C7), 69.9 (C13), 57.2 (C14),

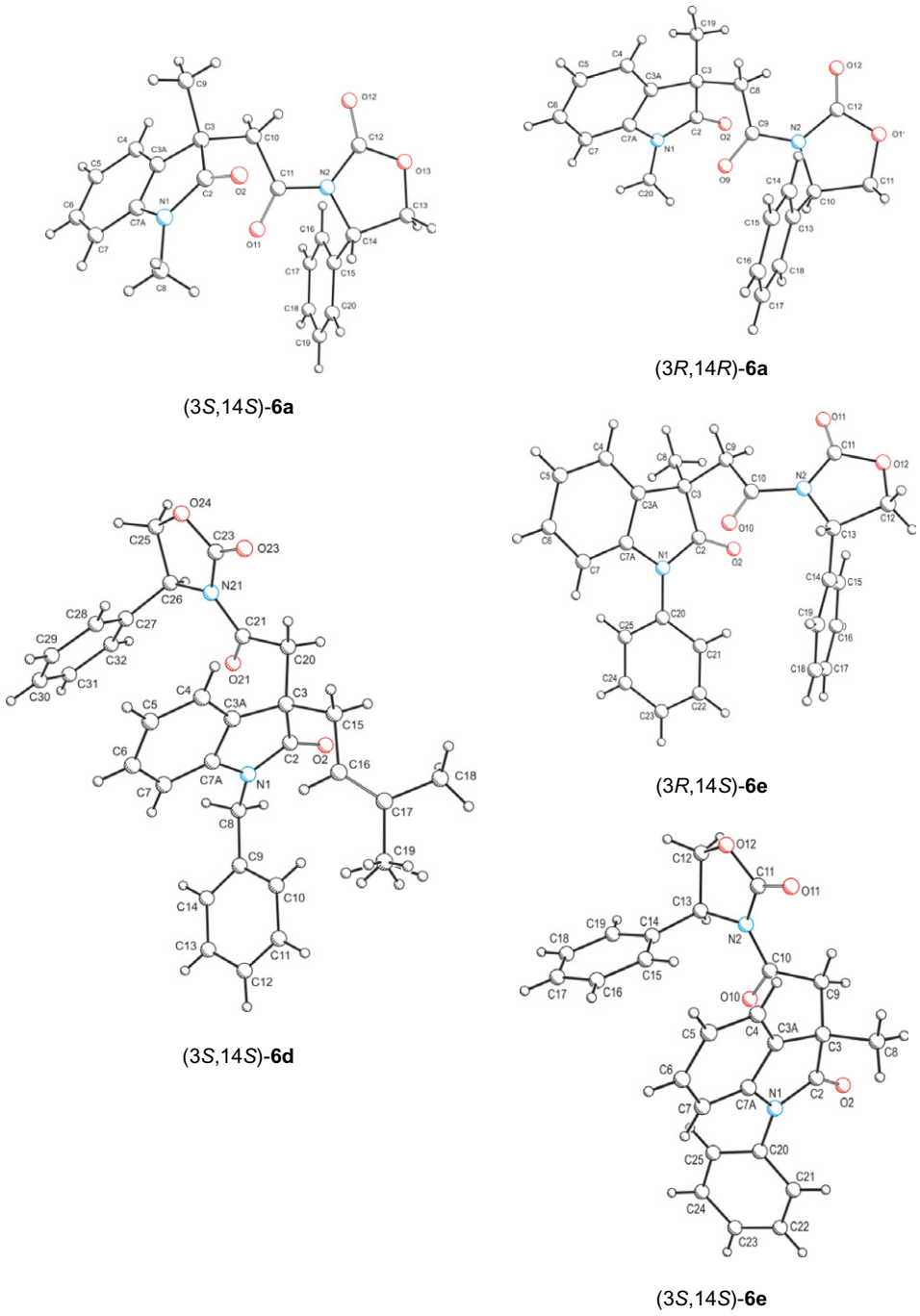

Figure 9. X-ray diffraction structures of (3*S*,14*S*)-**6a**, (3*R*,14*R*)-**6a**, (3*S*,14*S*)-**6d**, (3*R*,14*S*)-**6e** and (3*S*,14*S*)-**6e**.

50.0 (C3), 40.8 (C8), 38.0 (C21), 36.8 (C26), 25.8 (C29), 25.5 (C25), 18.0 (C24), 17.9 (C30); IR (film) ν_{max} 3057, 3033, 2917, 2856, 1781, 1709, 1611, 1489, 1467, 1456 cm^{-1}; EIMS *m*/*z* (relative intensity) 472 ([M]$^+$, 8), 404 (100), 267 (49), 241 (51), 185 (16), 172 (14), 158 (12), 145 (13); FABHRMS *m*/*z* calcd for $C_{29}H_{32}N_2O_4$ (M^+): 472.2362, found: 472.2361.

4.2.9. (*S*)-3-(2-((*R*)-1-Benzyl-3-(3-methylbut-2-enyl)-2-oxoindolin-3-yl)acetyl)-4-phenyloxazolidin-2-one (3*R*,14*S*)-6d

Prepared from **5d** as a yellow solid (0.30 g, 43%), mp: 74–75 °C. $[\alpha]_D^{20} = +119.8$ (*c* 1.09, $CHCl_3$). ^{1}H NMR (300 MHz, $CDCl_3$): δ 7.37–7.10 (11H, m, H4, H16–H20, H23–H27), 7.08 (1H, td, *J* = 7.8, 1.3 Hz, H6), 6.93 (1H, td, *J* = 7.5, 0.9 Hz, H5), 6.60 (1H, br d, *J* = 7.6 Hz, H7), 5.12 (1H, dd, *J* = 8.6, 3.6 Hz, H14), 4.88 and 4.77 (2H, AB, *J* = 15.9 Hz, H21), 4.84 (1H, tsp, *J* = 7.8, 1.4 Hz, H29), 4.46 (1H, br t, *J* = 8.7 Hz, H13A), 4.11 (1H, dd, *J* = 8.9, 3.7 Hz, H13B), 3.95 and 3.49 (2H, AB, *J* = 17.7 Hz, H8), 2.53 (2H, d, *J* = 7.6 Hz, H28), 1.58 (3H, d, *J* = 0.7 Hz, H31), 1.50 (3H, d, *J* = 1.0 Hz, H32); ^{13}C NMR (75 MHz, $CDCl_3$): δ 179.0 (C2), 168.7 (C9), 153.8 (C11), 143.4 (C7a), 138.4 (C15), 136.3 (C30), 136.0 (C22), 131.4 (C3a), 129.0 (2C, C17, C19), 128.5 (C18), 128.4 (2C, C24, C26), 127.7 (C6), 127.2 (2C, C23, C27), 127.1 (C25), 125.6 (2C, C16, C20), 122.1 (C4), 121.8 (C5), 116.9 (C29), 108.8 (C7), 69.9 (C13), 57.1 (C14), 49.7 (C3), 43.7 (C21), 41.2 (C8), 36.9 (C28), 25.8 (C31), 17.9 (C32); IR (film) ν_{max} 3061, 3031, 2972, 2917, 2857, 1780, 1710, 1614, 1490, 1466, 1456 cm^{-1}; EIMS *m*/*z* (relative intensity)

Table 4
Crystal data for (3*S*,14*S*)-**6a**, (3*R*,14*R*)-**6a**, (3*S*,14*S*)-**6d**, (3*R*,14*S*)-**6e** and (3*S*,14*S*)-**6e**

	(3*S*,14*S*)-**6a**	(3*R*,14*R*)-**6a**	(3*S*,14*S*)-**6d**	(3*R*,14*S*)-**6e**	(3*S*,14*S*)-**6e**
Empirical formula	$C_{21}H_{20}N_2O_4$	$C_{21}H_{20}N_2O_4$	$C_{31}H_{30}N_2O_4$	$C_{26}H_{22}N_2O_4$	$C_{26}H_{22}N_2O_4$
Formula weight	364.39	364.39	494.57	426.46	426.46
Crystal size (mm)	0.40 × 0.38 × 0.20	0.36 × 0.28 × 0.16	0.38 × 0.32 × 0.32	0.13 × 0.35 × 0.6	0.35 × 0.33 × 0.12
Wavelength (Å)	1.54184	1.54184	1.54184	0.71073	1.54184
Crystal system	Orthorhombic	Orthorhombic	Monoclinic	Orthorhombic	Orthorhombic
Space group	$P2_12_12_1$	$P2_12_12_1$	$P2_1$	$P2_12_12_1$	$P2_12_12$
Unit cell dimensions (Å)					
a	6.874(1)	6.862(5)	7.1305(9)	6.8409(1)	21.7953(6)
b	13.117(3)	13.123(2)	11.015(1)	11.8744(2)	15.0159(3)
c	20.458(4)	20.484(1)	16.860(4)	25.5360(4)	6.5806(2)
β (°)	90	90	93.8(1)	90	90
Volume (Å^3)	1844.7(6)	1844.0(1)	1321.3(4)	2074.33(6)	2153.7(1)
Z, Calculated density (mg/mm^3)	4, 1.312	4, 1.312	2, 1.243	4, 1.366	4, 1.315
Absorption coefficient (mm^{-1})	0.751	0.751	0.661	0.093	0.727
F(000)	768	768	524	896	896
θ Range for data collection (°)	4.32–59.87	4.32–59.97	2.53–59.95	1.59–26.26	3.57–73.74
Limiting indices	$0 \leqslant h \leqslant 7$, $0 \leqslant k \leqslant 14$, $2 \leqslant l \leqslant 22$	$0 \leqslant h \leqslant 7$, $0 \leqslant k \leqslant 14$, $-2 \leqslant l \leqslant 22$	$-8 \leqslant h \leqslant 7$, $0 \leqslant k \leqslant 12$, $0 \leqslant l \leqslant 18$	$-8 \leqslant h \leqslant 8$, $0 \leqslant k \leqslant 14$, $0 \leqslant l \leqslant 31$	$-26 \leqslant h \leqslant 26$, $-18 \leqslant k \leqslant 18$, $-6 \leqslant l \leqslant 7$
Collected reflections	1477 [*R*(int) = 0.0001]	1497 [*R*(int) = 0.0001]	2223 [*R*(int) = 0.0001]	16,832 [*R*(int) = 0.0001]	19,893 [*R*(int) = 0.0255]
Unique reflections	1411	1422	2064	4109	4261
Completeness to θ (%)	87.9	88.2	88.4	98.6	98.6
Data/restraints/parameters	1356/0/248	1294/0/248	1956/0/342	3927/0/295	3656/0/294
Goodness-of-fit on F^2	1.058	1.060	1.048	1.033	1.085
Final *R* indices [$I > 2\sigma(I)$] (%)	*R*1 = 3.4, *wR*2 = 8.9	*R*1 = 3.5, *wR*2 = 9.2	*R*1 = 3.1, *wR*2 = 8.9	*R*1 = 2.7, *wR*2 = 6.1	*R*1 = 3.8, *wR*2 = 8.6
R indices (all data) (%)	*R*1 = 3.4, *wR*2 = 9.6	*R*1 = 4.0, *wR*2 = 9.5	*R*1 = 3.3, *wR*2 = 9.0	*R*1 = 2.9, *wR*2 = 6.3	*R*1 = 4.8, *wR*2 = 9.2
Largest diff. peak and hole (e Å^3)	0.111 and −0.092	0.108 and −0.118	0.097 and −0.083	0.156 and −0.146	0.138 and −0.180
CCDC No.	858993	858994	858995	858996	858997

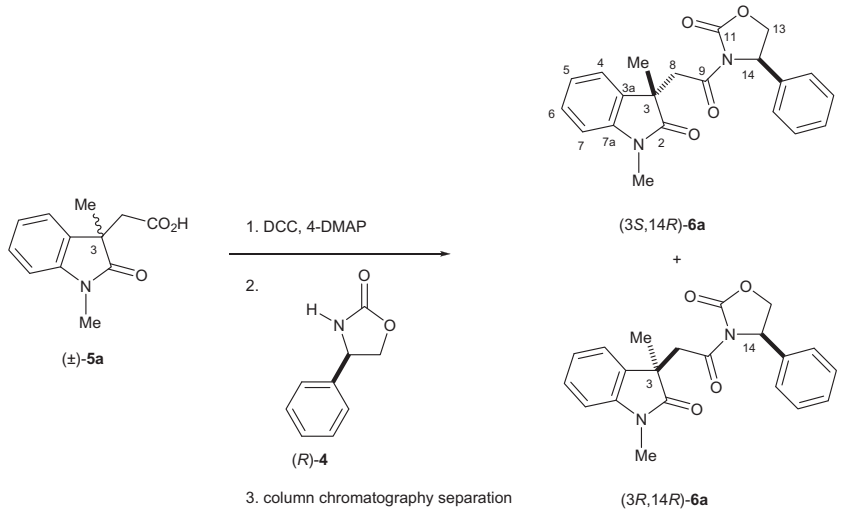

Scheme 3.

494 ([M]$^+$, 1), 428 (28), 426 (100), 290 (35), 264 (34), 263 (20), 236 (19), 91 (34); FABHRMS *m*/*z* calcd for $C_{31}H_{30}N_2O_4$ ([M]$^+$): 494.2206, found: 494.2197.

4.2.10. (*S*)-3-(2-((*S*)-1-Benzyl-3-(3-methylbut-2-enyl)-2-oxoindolin-3-yl)acetyl)-4-phenyoxazolidin-2-one (3*S*,14*S*)-6d

Prepared from **5d** as white crystals (0.30 g, 43%), mp: 173–174 °C (EtOAc/hexane). $[\alpha]_D^{20} = +63.7$ (*c* 1.75, $CHCl_3$). ^{1}H NMR (300 MHz, $CDCl_3$): δ 7.24–7.09 (9H, m, H4, H17–H19, H23–H27), 7.05 (1H, td, *J* = 7.8, 1.3 Hz, H6), 6.93 (1H, td, *J* = 7.5, 1.0 Hz, H5), 6.79 (2H, m, H16, H20), 6.48 (1H, br d, *J* = 7.5 Hz, H7), 5.26 (1H, dd, *J* = 8.6, 3.7 Hz, H14), 5.06 and 4.64 (2H, AB, *J* = 16.0 Hz, H21), 4.84 (1H, tsp, *J* = 7.6, 1.4 Hz, H29), 4.57 (1H, t, *J* = 8.7 Hz, H13A), 4.17 and 3.37 (2H, AB, *J* = 16.7 Hz, H8), 4.09 (1H, dd, *J* = 8.8, 3.7 Hz, H13B), 2.55 (2H, d, *J* = 7.6 Hz, H28), 1.57 (3H, d, *J* = 0.9 Hz, H31), 1.49 (3H, d, *J* = 1.2 Hz, H32); ^{13}C NMR (75 MHz, $CDCl_3$): δ 179.2 (C2), 168.8 (C9), 153.7 (C11), 143.4 (C7a), 138.2 (C15), 136.3 (C30), 136.0 (C22), 130.8 (C3a), 128.8 (C17, C19), 128.5 (C24, C26), 128.0 (C18), 127.8 (C6), 127.1 (C25), 127.0 (C23, C27), 125.0 (C16, C20), 122.5 (C4), 121.8 (C5), 116.9 (C29), 109.0 (C7), 69.9 (C13), 57.2 (C14), 50.2 (C3), 43.7 (C21), 40.6 (C8), 37.0 (C28), 25.8 (C31), 18.0 (C32); IR (film) ν_{max} 3060, 3034, 2919,

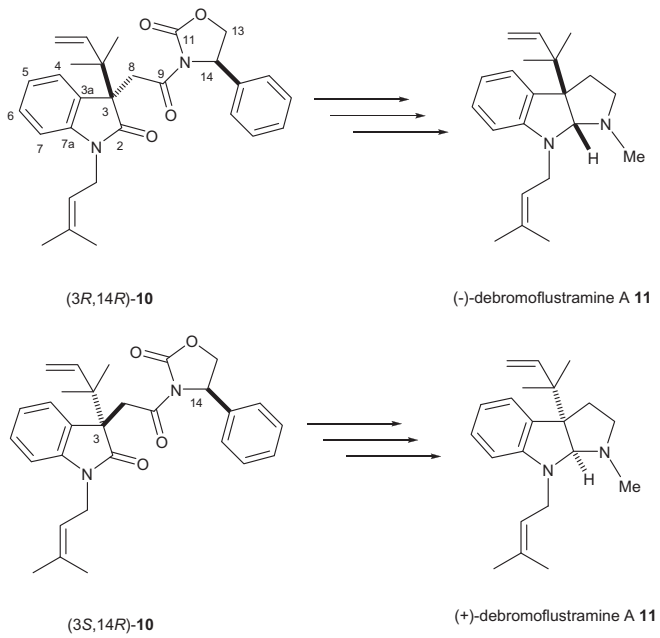

Scheme 4.

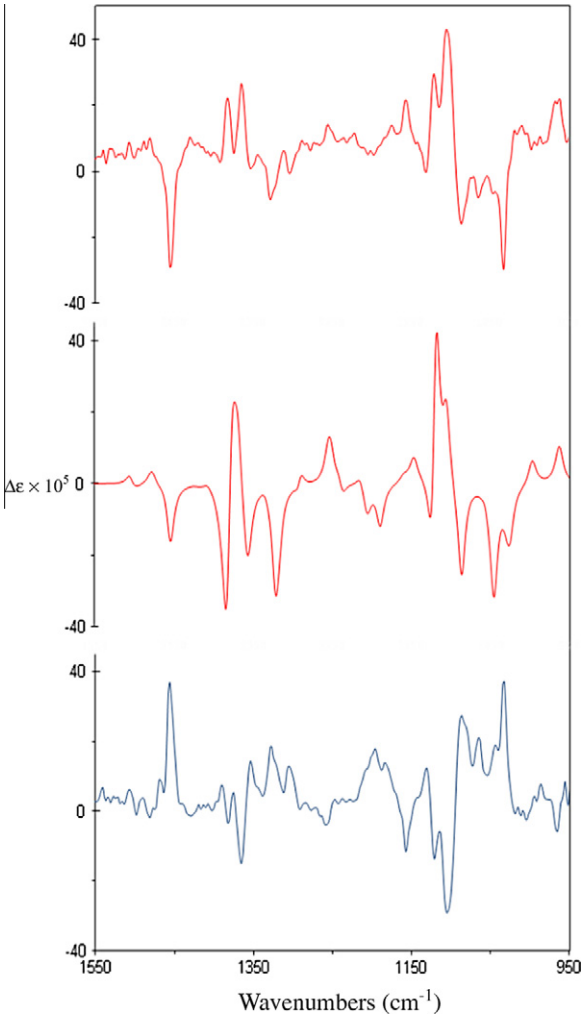

Figure 10. Comparison of the B3PW91/DGDZVP2 calculated (center) VCD spectrum of (3*S*,14*S*)-**6a** and the experimental VCD spectra of (3*S*,14*S*)-**6a** (top) and its enantiomer (3*R*,14*R*)-**6a** (bottom).

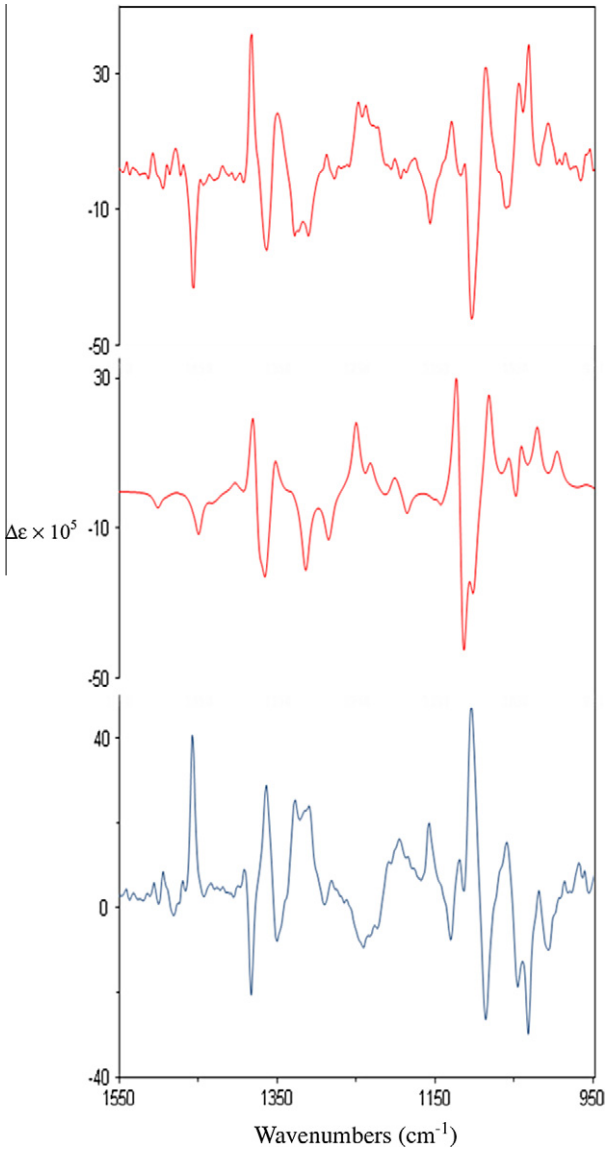

Figure 11. Comparison of the B3PW91/DGDZVP2 calculated (center) VCD spectrum of (3*R*,14*S*)-**6a** and the experimental VCD spectra of (3*R*,14*S*)-**6a** (top) and its enantiomer (3*S*,14*R*)-**6a** (bottom).

1780, 1712, 1489, 1467, 1456 cm^{-1}; EIMS *m/z* (relative intensity) 494 ($[M]^+$, 7), 426 (100), 290 (32), 289 (33), 263 (36), 262 (20), 235 (44), 91 (51); FABHRMS *m/z* calcd for $C_{31}H_{30}N_2O_4$ ($[M]^+$): 494.2206, found: 494.2206.

4.2.11. (*S*)-3-(2-((*R*)-3-Methyl-2-oxo-1-phenylindolin-3-yl)-acetyl)-4-phenyloxazolidin-2-one (3*R*,14*S*)-6e

Prepared from **5e** as white crystals (0.021 g, 14%), mp: 168–169 °C (MeOH). $[\alpha]_D^{20} = +166.3$ (*c* 2.0, $CHCl_3$). ^1H NMR (400 MHz, $CDCl_3$): δ 7.43 (2H, br t, *J* = 7.4 Hz, H23, H25), 7.39–7.28 (4H, m, H17–H19, H24), 7.27–7.13 (5H, H4, H16, H20, H22, H26), 7.17 (1H, td, *J* = 7.8, 1.1 Hz, H6), 7.04 (1H, td, *J* = 7.4, 0.8 Hz, H5), 6.76 (1H, br d, *J* = 7.8 Hz, H7), 5.22 (1H, dd, *J* = 8.6, 3.9 Hz, H14), 4.57 (1H, t, *J* = 8.8 Hz, H13A), 4.20 (1H, dd, *J* = 9.0, 3.9 Hz, H13B), 3.93 and 3.52 (2H, AB, *J* = 17.6 Hz, H8), 1.50 (3H, s, H27); ^{13}C NMR (100 MHz, $CDCl_3$): δ 179.7 (C2), 169.2 (C9), 154.2 (C11), 144.2 (C7a), 138.7 (C15), 135.2 (C21), 133.5 (C3a), 129.8 (2C, C23, C25), 129.4 (2C, C17, C19), 128.9 (C18), 128.2 (C6, C24), 127.2 (2C, C22, C26), 126.1 (2C, C16, C20), 122.9

(C5), 122.3 (C4), 109.6 (C7), 70.4 (C13), 57.7 (C14) 45.8 (C3), 43.4 (C8), 25.1 (C27); IR (KBr) ν_{max} 3032, 2970, 2926, 1779, 1713, 1612, 1501, 1482, 1384, 1363 cm^{-1}; EIMS *m/z* (relative intensity) 426 ([M]$^+$, 100), 249 (11), 237 (49), 223 (14), 77 (8), 51 (5); FAB-HRMS *m/z* calcd for $C_{26}H_{23}N_2O_4$ ([M+1]$^+$): 427.1658, found: 427.1660.

4.2.12. (*S*)-3-(2-((*S*)-3-Methyl-2-oxo-1-phenylindolin-3-yl)-acetyl)-4-phenyloxazolidin-2-one (3*S*,14*S*)-6e

Prepared from **5e** as white crystals (0.023 g, 15%), mp: 181–182 °C (MeOH). $[\alpha]_D^{20} = +200.0$ (*c* 2.0, $CHCl_3$). ^{1}H NMR (400 MHz, $CDCl_3$): δ 7.45 (2H, br t, *J* = 7.7 Hz, H23, H25), 7.35 (1H, br t, *J* = 7.5 Hz, H24), 7.30–7.25 (3H, m, H4, H22, H26), 7.18–7.15 (3H, m, H17–H19), 7.11 (1H, td, *J* = 7.7, 1.4 Hz, H6), 7.02 (1H, td, *J* = 7.4, 0.7 Hz, H5), 6.85 (2H, m, H16, H20), 6.62 (1H, br d, *J* = 7.8 Hz, H7), 5.28 (1H, dd, *J* = 8.6, 3.5 Hz, H14), 4.59 (1H, t, *J* = 8.6 Hz, H13A), 4.12 (1H, dd, *J* = 9.0, 3.6 Hz, H13B), 4.16 and 3.39 (2H, AB, *J* = 16.9 Hz, H8), 1.51 (3H, s, H27); ^{13}C NMR (100 MHz, $CDCl_3$): δ 179.8 (C2), 169.0 (C9), 154.1 (C11), 144.1 (C7a), 138.6 (C15), 135.1 (C21), 132.8 (C3a), 129.7 (2C, C23, C25), 129.2 (2C, C17,19), 128.4 (C18), 128.2, 128.1 (2C, C6, C24), 127.1 (2C, C22, C26), 125.5 (2C, C16, C20), 122.9 (C5), 122.6 (C4), 109.8 (C7), 70.3 (C13), 57.6 (C14) 46.2 (C3), 42.6 (C8), 25.1 (C27); IR (KBr) ν_{max} 2919, 1779, 1716, 1612, 1596, 1502, 1482, 1467, 1455, 1384, 1363, 1330, 1303, 1204 cm^{-1}; EIMS *m/z* (relative intensity) 426 ([M]$^+$, 100), 249 (8), 237 (39), 223 (8), 77 (8), 51 (7); FABHRMS *m/z* calcd for $C_{26}H_{23}N_2O_4$ ([M+1]$^+$): 427.1658, found: 427.1654.

4.3. VCD measurements

VCD spectra were measured using a BioTools BOMEM Chiral*IR* spectrophotometer equipped with a dual photoelastic modulation. Samples of diastereomers (3*S*,14*S*)-**6a**, (3*R*,14*S*)-**6a**, (3*R*,14*R*)-**6a,** and (3*S*,14*R*)-**6a** were dissolved in 150 μL of $CDCl_3$, placed in a BaF_2 cell with a path length of 100 μm and data were acquired at a resolution of 4 cm^{-1} during 4 h. For (3*S*,14*S*)-**6a**, (3*R*,14*R*)-**6a** and (3*S*,14*R*)-**6a** 5.0 mg were used, while for (3*R*,14*S*)-**6a**, 5.2 mg were measured. Baseline corrections were done either by subtracting the individual spectra of (3*S*,14*S*)-**6a**, (3*R*,14*S*)-**6a**, (3*R*,14*R*)-**6a,** and (3*S*,14*R*)-**6a** from the solvent or from a 5 mg samples of their respective racemic mixture in 150 μL of $CDCl_3$.

4.4. X-ray diffraction analyses

Data collections for (3*S*,14*S*)-**6a**, (3*R*,14*R*)-**6a** and (3*S*,14*S*)-**6d** were carried out on a Bruker-Nonius CAD4 diffractometer while those for (3*R*,14*S*)-**6e** and (3*S*,14*S*)-**6e** were done on a Agilent Technologies Gemini A CCD diffractometer using Cu/Kα radiation (λ = 1.54184 Å). The structures were solved by direct methods using the SHELXS-97[24] program included in the WINGX v1.6 package.[25] Structural refinements were carried out by full-matrix least squares on *F*2. The non-hydrogen atoms were treated anisotropically, and the hydrogen atoms, included in the structure factor calculation, were refined isotropically. Atomic coordinates, bond lengths, bond angles, and anisotropic thermal parameters are in deposit at the Cambridge Crystallographic Data Center. Table 4 summarizes the relevant data.

Acknowledgments

We are pleased to acknowledge the financial support from CONACYT (Mexico) grants 83723 and 84453. L.E.C.D. and E.A.Z.E. thank CONACYT for fellowships 186031, 58994 (for L.E.C.D.) and 237631 (for E.Z.E.).

References

1. (a) Kinashi, H.; Suzuki, Y.; Takeuchi, S.; Kawarada, A. *Agric. Biol. Chem.* **1976**, *40*, 2465–2470; (b) Suzuki, Y.; Kinashi, H.; Takeuchi, S.; Kawarada, A. *Phytochemistry* **1977**, *16*, 635–637; (c) Ohmoto, T.; Yamaguchi, K.; Ikeda, K. *Chem. Pharm. Bull.* **1988**, *36*, 578–581; (d) Dekker, T. G.; Fourie, T. G.; Matthee, E.; Snyckers, F. O. *Phytochemistry* **1987**, *26*, 1845–1846; (e) Monde, K.; Sasaki, K.; Shirata, A.; Takasugi, M. *Phytochemistry* **1991**, *30*, 2915–2917; (f) Zhang, H.-p.; Kamano, Y.; Ichihara, Y.; Kizu, H.; Komiyama, K.; Itokawa, H.; Pettit, G. R. *Tetrahedron* **1995**, *51*, 5523–5528; (g) Fréchard, A.; Fabre, N.; Péan, C.; Montaut, S.; Fauvel, M.-T.; Rollin, P.; Fourasté, I. *Tetrahedron Lett.* **2001**, *42*, 9015–9017; (h) Emura, T.; Esaki, T.; Tachibana, K.; Shimizu, M. *J. Org. Chem.* **2006**, *71*, 8559–8564.
2. (a) Morales-Ríos, M. S.; Suárez-Castillo, O. R.; Joseph-Nathan, P. *Trends Heterocycl. Chem.* **1999**, *6*, 111–124; (b) Horne, S.; Taylor, N.; Collins, S.; Rodrigo, R. *J. Chem. Soc., Perkin Trans. 1* **1991**, 3047–3051; (c) Yu, Q.-s.; Luo, W.-m.; Li, Y.-q. *Heterocycles* **1993**, *36*, 1279–1285; (d) Pallavicini, M.; Valoti, E.; Villa, L.; Resta, I. *Tetrahedron: Asymmetry* **1994**, *5*, 363–370; (e) Pei, X.-F.; Bi, S. *Heterocycles* **1994**, *39*, 357–360; (f) Matsuura, T.; Overman, L. E.; Poon, D. J. *J. Am. Chem. Soc.* **1998**, *120*, 6500–6503; (g) Morales-Ríos, M. S.; Suárez-Castillo, O. R. *Nat. Prod. Commun.* **2008**, *3*, 629–642; (h) Kawasaki, T.; Terashima, R.; Sakaguchi, K.-e.; Sekiguchi, H.; Sakamoto, M. *Tetrahedron Lett.* **1996**, *37*, 7525–7528; (i) Morales-Ríos, M. S.; Rivera-Becerril, E.; Joseph-Nathan, P. *Tetrahedron: Asymmetry* **2005**, *16*, 2493–2499; (j) Suárez-Castillo, O. R.; Sánchez-Zavala, M.; Meléndez-Rodríguez, M.; Castelán-Duarte, L. E.; Morales-Ríos, M. S.; Joseph-Nathan, P. *Tetrahedron* **2006**, *62*, 3040–3051; (k) Suárez-Castillo, O. R.; Sánchez-Zavala, M.; Meléndez-Rodríguez, M.; Aquino-Torres, E.; Morales-Ríos, M. S.; Joseph-Nathan, P. *Heterocycles* **2007**, *71*, 1539–1551; (l) Kawasaki, T.; Shinada, M.; Kamimura, D.; Ohzono, M.; Ogawa, A. *Chem. Commun.* **2006**, 420–422.
3. Suárez-Castillo, O. R.; Meléndez-Rodríguez, M.; Castelán-Duarte, L. E.; Sánchez-Zavala, M.; Rivera-Becerril, E.; Morales-Ríos, M. S.; Joseph-Nathan, P. *Tetrahedron: Asymmetry* **2009**, *20*, 2374–2389.
4. (a) Kouko, T.; Matsumura, K.; Kawasaki, T. *Tetrahedron* **2005**, *61*, 2309–2318; (b) Boteju, L. W.; Wegner, K.; Qian, X.; Hruby, J. V. *Tetrahedron* **1994**, *50*, 2391–2404; (c) Davies, S. G.; Sanganee, H. J. *Tetrahedron: Asymmetry* **1995**, *6*, 671–674; (d) Palomo, C.; Aizpurua, J. M.; Mielgo, A.; Linden, A. *J. Org. Chem.* **1996**, *61*, 9186–9195; (e) Hosokawa, T.; Yamanaka, T.; Itotani, M.; Murahashi, S.-I. *J. Org. Chem.* **1995**, *60*, 6159–6167; (f) Akiba, T.; Tamura, O.; Hashimoto, M.; Kobayashi, Y.; Katoh, T.; Nakatani, K.; Kamada, M.; Hayakawa, I.; Terashima, S. *Tetrahedron* **1994**, *50*, 3905–3914; (g) Davies, I. W.; Senanayake, C. H.; Castonguay, L.; Larsen, R. D.; Verhoeven, T. R.; Reider, P. J. *Tetrahedron Lett.* **1995**, *36*, 7619–7622.
5. (a) Pirkle, W. H.; Simmons, K. A. *J. Org. Chem.* **1983**, *48*, 2520–2527; (b) Pridgen, L. N.; De Brosse, C. *J. Org. Chem.* **1997**, *62*, 216–220.
6. (a) Morales-Ríos, M. S.; Rivera-Becerril, E.; González-Juárez, D. E.; García-Vázquez, J. B.; Trujillo-Serrato, J. J.; Hernández-Barragán, A.; Joseph-Nathan, P. *Nat. Prod. Commun.* **2011**, *6*, 457–464; (b) Lakshmaiah, G.; Kawabata, T.; Shang, M.; Fuji, K. *J. Org. Chem.* **1999**, *64*, 1699–1704; (c) Miyamoto, H.; Okawa, Y.; Nakazaki, A.; Kobayashi, S. *Tetrahedron Lett.* **2007**, *48*, 1805–1808; (d) Walker, G. N.; Alkalay, D.; Smith, R. T. *J. Org. Chem.* **1965**, *30*, 2973–2983.
7. (a) Trost, B. M.; Belletire, J. L.; Godleski, S.; McDougal, P. G.; Balkovec, J. M. *J. Org. Chem.* **1986**, *51*, 2370–2374; (b) Hori, K.; Hikage, N.; Inagaki, A.; Mori, S.; Nomura, K.; Yoshii, E. *J. Org. Chem.* **1992**, *57*, 2888–2902.
8. Yabuuchi, T.; Kusumi, T. *J. Org. Chem.* **2000**, *65*, 397–404.
9. Shaye, N. A.; Eames, J. *Tetrahedron Lett.* **2010**, *51*, 5892–5895.
10. (a) Osman, F. H.; El-Samahy, F. A. *Phosphorus, Sulfur Silicon* **1998**, *134/135*, 437–446; (b) Aldrich/ACD Library of FT NMR Spectra Pro. Advanced Chemistry Development, Inc. and Aldrich Chemical Company, Inc. V. 1.00, 1998.
11. Taaning, R. H.; Lindsay, K. B.; Schiøtt, B.; Daasbjerg, K.; Skrydstrup, T. *J. Am. Chem. Soc.* **2009**, *131*, 10253–10262.
12. Kitoh, S.; Senda, H.; Kunimoto, K.-K.; Maeda, S.; Kuwae, A.; Hanai, K. *Cryst. Res. Technol.* **2004**, *39*, 375–381.
13. Chang, G.; Guida, W. C.; Still, W. C. *J. Am. Chem. Soc.* **1989**, *111*, 4379–4386.
14. Hehre, W. J.; Radom, L.; Schleyer, P. v. R.; Pople, J. A. *Ab Initio Molecular Orbital Theory*; Wiley: New York, 1986.
15. (a) Godbout, N.; Salahub, D. R.; Andzelm, J.; Wimmer, E. *Can. J. Chem.* **1992**, *70*, 560–571; (b) Andzelm, J.; Wimmer, E. *J. Chem. Phys.* **1992**, *96*, 1280–1303.
16. (a) Cheeseman, J. R.; Trucks, G. W.; Keith, T. A.; Frisch, M. J. *J. Chem. Phys.* **1996**, *104*, 5497–5509; (b) Cerda-García-Rojas, C. M.; Catalán, C. A. N.; Muro, A. C.; Joseph-Nathan, P. *J. Nat. Prod.* **2008**, *71*, 967–971.
17. (a) Halgren, T. A. *J. Comput. Chem.* **1996**, *17*, 490–519; (b) Halgren, T. A. *J. Comput. Chem.* **1996**, *17*, 520–552; (c) Halgren, T. A. *J. Comput. Chem.* **1996**, *17*, 553–586; (d) Halgren, T. A.; Nachbar, R. B. *J. Comput. Chem.* **1996**, *17*, 587–615; (e) Halgren, T. A. *J. Comput. Chem.* **1996**, *17*, 616–641.
18. As implemented in the computer package SPARTAN04, Windows v 1.0.1; Wavefunction Inc.: Irvine, CA, USA, 2004.
19. Frisch, M. J.; Trucks, G. W.; Schlegel, H. B.; Scuseria, G. E.; Robb, M. A.; Cheeseman, J. R.; Montgomery, J. A., Jr.; Vreven, T.; Kudin, K. N.; Burant, J. C.; Millam, J. M.; Iyengar, S. S.; Tomasi, J.; Barone, V.; Mennucci, B.; Cossi, M.; Scalmani, G.; Rega, N.; Petersson, G. A.; Nakatsuji, H.; Hada, M.; Ehara, M.; Toyota, K.; Fukuda, R.; Hasegawa, J.; Ishida, M.; Nakajima, T.; Honda, Y.; Kitao, O.; Nakai, H.; Klene, M.; Li, X.; Knox, J. E.; Hratchian, H. P.; Cross, J. B.; Bakken, V.; Adamo, C.; Jaramillo, J.; Gomperts, R.; Stratmann, R. E.; Yazyev, O.; Austin, A. J.; Cammi, R.; Pomelli, C.; Ochterski, J. W.; Ayala, P. Y.; Morokuma, K.; Voth, G.

A.; Salvador, P.; Dannenberg, J. J.; Zakrzewski, V. G.; Dapprich, S.; Daniels, A. D.; Strain, M. C.; Farkas, O.; Malick, D. K.; Rabuck, A. D.; Raghavachari, K.; Foresman, J. B.; Ortiz, J. V.; Cui, Q.; Baboul, A. G.; Clifford, S.; Cioslowski, J.; Stefanov, B. B.; Liu, G.; Liashenko, A.; Piskorz, P.; Komaromi, I.; Martin, R. L.; Fox, D. J.; Keith, T.; Al-Laham, M. A.; Peng, C. Y.; Nanayakkara, A.; Challacombe, M.; Gill, P. M. W.; Johnson, B.; Chen, W.; Wong, M. W.; Gonzalez, C.; Pople, J. A.; Gaussian, Inc.: Wallingford CT, 2004.

20. Kawasaki, T.; Shinada, M.; Ohzono, M.; Ogawa, A.; Terashima, R.; Sakamoto, M. *J. Org. Chem.* **2008**, *73*, 5959–5964.
21. Nakahashi, A.; Yaguchi, Y.; Miura, N.; Emura, M.; Monde, K. *J. Nat. Prod.* **2011**, *74*, 707–711.
22. Zepeda, L. G.; Burgueño-Tapia, E.; Joseph-Nathan, P. *Nat. Prod. Commun.* **2011**, *6*, 429–432.
23. Debie, E.; De Gussem, E.; Dukor, R. K.; Herrebout, W.; Nafie, L. A.; Bultinck, P. *Chem. Phys. Chem.* **2011**, *12*, 1542–1549.
24. Sheldrick, G. M. *Programs for Crystal Structure Analysis*; Institüt für Anorganische Chemie der Universität, University of Göttingen: Göttingen, Germany, 1988.
25. Farrugia, L. J. *J. Appl. Crystallogr.* **1999**, *32*, 837–838.